EXPERIMENTAL CHARACTERIZATION OF SOME WATER SOLUBLE POLYMERS USED IN DRILLING AND COMPLETION FLUIDS

A THESIS SUBMITTED TO
THE GRADUATE SCHOOL OF NATURAL AND APPLIED SCIENCES
OF
MIDDLE EAST TECHNICAL UNIVERSITY

BY

BERKAY GÜRBÜZ

IN PARTIAL FULFILLMENT OF THE REQUIREMENTS
FOR
THE DEGREE MASTER OF SCIENCE
IN
PETROLEUM AND NATURAL GAS ENGINEERING

FEBRUARY 2012

Approval of the thesis:

EXPERIMENTAL CHARACTERIZATION OF SOME WATER SOLUBLE POLYMERS USED IN DRILLING AND COMPLETION FLUIDS

submitted by **BERKAY GÜRBÜZ** in partial fulfillment of the requirements for the degree of **Master of Science in Petroleum and Natural Gas Engineering Department, Middle East Technical University** by,

Prof. Dr. Canan ÖZGEN ____________________
Dean, Graduate School of Natural and Applied Sciences**,**

Prof. Dr. Mahmut PARLAKTUNA ____________________
Head of Dept., Petroleum and Nat.Gas Eng. Dept., METU

Prof. Dr. M. Tanju MEHMETOĞLU ____________________
Supervisor, Petroleum and Natural Gas Eng. Dept., METU

Assoc. Prof. Dr. İ. Hakkı GÜCÜYENER ____________________
Co Supervisor, KARKİM, ANKARA

Examining Committee Members

Prof. Dr. Mahmut PARLAKTUNA ____________________
Petroleum and Natural Gas Engineering Dept., METU

Prof. Dr. M. Tanju MEHMETOĞLU ____________________
Petroleum and Natural Gas Engineering Dept., METU

Prof. Dr. Nurkan KARAHANOĞLU ____________________
Geological Engineering Dept., METU

Asst. Prof. Dr. Çağlar SINAYUÇ ____________________
Petroleum and Natural Gas Engineering Dept., METU

Assoc. Prof. Dr. İ. Hakkı GÜCÜYENER ____________________
KARKİM, ANKARA

Date: 10/02/2012

I hereby declare that all information in this document has been obtained and presented in accordance with academic rules and ethical conduct. I also declare that, as required by these rules and conduct, I have fully cited and referenced all material and results that are not original to this work.

Name, Last name : Berkay GÜRBÜZ

Signature :

ABSTRACT

EXPERIMENTAL CHARACTERIZATION OF SOME WATER SOLUBLE POLYMERS USED IN DRILLING AND COMPLETION FLUIDS

Gürbüz, Berkay
M.S., Department of Petroleum and Natural Gas Engineering
Supervisor: Prof. Dr. M. Tanju Mehmetoğlu
Co-Supervisor: Assoc. Prof. Dr. İ. Hakkı Gücüyener

February 2012, 85 Pages

Properly preparing the drilling fluid is an essential part of any successful drilling operation, especially in complex operations like deviated and horizontal drilling. Understanding the flow behavior of the polymers used in the drilling fluids under different conditions takes a key part in this preparation. In this study, shear rheology of some traditionally used water soluble polymers in drilling and completion fluids; namely PAC (poly anionic cellulose) and xanthan gum, were investigated experimentally. Instead of an oilfield standard Fann Model 35 Viscometer, an Ofite Model 900 Viscometer was used because of its capability to measure at ultra-low shear rates. Effects of the concentration of the polymer, time of shear applied, test temperature and effects of aging were examined. Rheological measurements were conducted between the shear rate ranges of 0.01 to 1000s^{-1} with concentrations changing from 0.25 to 1.5 grams of polymer per 350 milliliters of water (equivalent to 0.25 to 1.5 lb/bbl). Rheograms were constructed to identify the effect the polymers in question have on the flow characteristics of the drilling fluid. An appropriate constitutive model was used to define the flow behavior of the polymer in question mathematically.

It was observed from the constructed rheograms that increase in polymer concentration results in consistent increase of apparent viscosity. Amount of time of shear does not affect the selected polymers if they are dynamically aged at least for two hours. Also as expected increasing temperature of the sample lowers the apparent viscosity considerably.

Keywords: rheology, drilling fluid, polymer, low shear rate viscosity

ÖZ

SONDAJ VE TAMAMLAMA SIVILARINDA KULLANILAN SUDA ÇÖZÜNÜR BAZI POLİMERLERİN DENEYSEL KARAKTERİZASYONU

Gürbüz, Berkay

Yüksek Lisans, Petrol ve Doğal Gaz Mühendisliği Bölümü

Tez Yöneticisi: Prof. Dr. M. Tanju Mehmetoğlu
Ortak Tez Yöneticisi: Doç. Dr. İ. Hakkı Gücüyener

Şubat 2012, 85 Sayfa

Özellikle yönlü ve yatay kuyu sondajları gibi karmaşık operasyonlarda sondaj sıvısının uygun şekilde hazırlanması hayati bir önem taşır. Sondaj sıvısını hazırlarken kullanılan polimerlerin farklı koşullarda akış davranışlarını anlamak sondaj sıvılarının hazırlanmasında anahtar bir noktadır. Bu çalışmada PAC (poli anyonik selüloz) ve XCD (ksantan sakızı), gibi sondaj ve tamamlama sıvılarında sıklıkla kullanılan bazı polimerlerin reolojileri deneysel olarak incelenmiştir. Çok düşük kayma hızlarında ölçüm yapma kabiliyetine sahip Ofite Model 900 Viskometre, saha standardı sayılan Fann Model 35 viskometrenin yerine kullanılmıştır. Kullanılan polimerin miktarı, kayma geriliminin uygulandığı süre, test sıcaklığı ve yaşlandırma süresinin etkileri incelenmiştir. Reolojik ölçümler 0.01–1000s^{-1} kayma hızları arasında 350 mililitre suya 0.25'ten 1.5 grama kadar (0.25 – 1.5 lb/bbl) değişen miktarlarda polimer eklenerek yapılmıştır. İncelenmekte olan polimerlerin sondaj sıvısının akış özellikleri üzerindeki etkisi reoloji eğrileri çizilerek incelenmiştir. Sondaj sıvısının akış davranışlarını matematiksel olarak tanımlamak için uygun bir reolojik model kullanılmıştır.

Oluşturulmuş olan reoloji eğrilerinden görüleceği üzere polimer miktarını arttırmak viskozite değerlerini düzenli olarak arttırmaktadır. Kayma geriliminin uygulandığı süredeki değişim ise, en az iki saat olmak şartı ile sondaj sıvısına yapılan yaşlandırma sonrası bir fark yaratmamaktadır. Ayrıca beklenildiği üzere test sıcaklıklarını arttırmak viskozite değerlerini gözle görülür bir şekilde düşürmektedir.

Anahtar Kelimeler: Reoloji, sondaj sıvısı, polimer, düşük kayma hızlarında viskozite

To My Parents…

ACKNOWLEDGEMENTS

I would like to express my deepest gratitude to my supervisor Prof. Dr. M. Tanju MEHMETOĞLU for the guidance, advice and criticism he provided throughout my research.

I wish to thank my co-supervisor Assoc. Prof. Dr. İ. Hakkı GÜCÜYENER for his guidance, encouragements and invaluable advice. He truly played an important role in each step of the research made and helped shape most of the thesis.

During my research period, I received help from my former colleagues in Middle East Technical University, Petroleum and Natural Gas Engineering Department. Especially Tuğçe BAYRAM, S. Aslı GÜNDOĞAR and Sevtaç BÜLBÜL deserve my sincerest thanks to the fullest.

Finally, special thanks to my family, the completion of this work would not be possible without their encouragement, understanding and endless patience.

TABLE OF CONTENTS

CHAPTERS

LIST OF FIGURES

FIGURES

LIST OF TABLES

TABLES

NOMENCLATURE

Abbreviations

API : American Petroleum Institute
CMC : Carboxymethyl cellulose
ECD : Equivalent circulating density
EMW : Equivalent mud weight
PAC : Poly anionic cellulose
XCD : Xanthan gum

Latin Symbols

C : Grams of polymer in 350 mg of distilled water (lb/bbl)
n : Flow behavior index
K : Consistency index
T : Temperature, °C or °F

Greek Symbols

τ : Shear stress, lb/100 ft^2
τ_y : Yield stress, lb/100 ft^2
γ : Shear rate, s^{-1}
μ_a : Apparent viscosity, cp
μ_p : Plastic viscosity, cp

CHAPTER 1

INTRODUCTION

Aim of the drilling operation is to reach commercially exploitable hydrocarbon resources present in reservoirs beneath Earth’s surface in the most economical way and in the shortest time possible. A drilling system has several components and drilling fluids have been an essential part of the drilling process since the start of the rotary drilling period. The main function of the drilling fluid is to remove the cuttings present in the wellbore, which is achieved by circulating the drilling fluid down the drill string, from bit nozzles and through the annulus back to the surface. Drilling fluids have secondary functions like providing hydrostatic pressure to stabilize the wellbore, providing a medium for formation logging operations, cooling and lubricating the bit, forming a filter cake to reduce the fluid loss, and transmitting power to the bit nozzles. Most of the drilling and completion fluids used in today’s world are complex mixtures of different interacting components. These mixtures are designed to fulfill many requirements and improve the drilling and completion processes as much as possible. Flow properties of these drilling fluid mixtures are linked to many important aspects during drilling and well completion operations, like predicting fluid pressure loss and equivalent circulating density, modeling annular velocity profiles for hole cleaning requirements in vertical and deviated wellbores, particle settling velocity estimation and determining suspension and transport properties for sag occurrence, providing hole stability and effecting swab pressures.

To design an appropriate drilling fluid for drilling or completion operations, rheological properties of the drilling fluid should be known in detail. Rheology describes the deformation of a body under the influence of stresses [1]. The body in this context is fluids, namely drilling fluids. Fluids respond to stress by flowing; the flow of a liquid includes the mass, the momentum and the energy change with respect to position and time. Fluid rheology in a drilling or completion operation focuses on the relation between shear rate and shear stress and the impact these two have on flow characteristics inside tubular and annular spaces. Every fluid responds to applied stress in different ways. Newton described a constant of proportionality, called viscosity, which is the relation between the rate of deformation and the applied stress. However, there are fluids which do not exhibit Newtonian characteristics, like drilling and completion fluids; meaning that there is not a linear relationship between their rate of deformation and the stress applied to them, and the word rheology was invented mainly for such fluids.

1.1 RHEOLOGICAL MODELS

Numerous different models, which try to mathematically describe the relationship between shear rate and shear stress of non-Newtonian liquids, have been developed over time. Generally drilling and completion fluids are optimized using mathematical models and viscosity is a parameter of utmost importance in these mathematical models. Viscosity is utilized to express the friction created because of the intermolecular attraction of the fluid when a stress is applied to actuate the fluid. Numerous additives are added to the formulation in order to reach optimized specific purposes which are sometimes contradictory. For example, mud has to be viscous enough in order to be able to lift cuttings to the surface, but at the same time, viscosity must not be too high in order to minimize friction pressure loss [2].

There are numerous different methods which have several constants, however due to the complexity of calculating the parameters they have not received any added interest. This study focuses on the commonly used two parameter models, Bingham Plastic and Power Law, and the three parameter Herschel-Bulkley model.

1.1.1 POWER LAW MODEL

Power Law or Ostwald de Waele Model is one of the simplest ways to present the relationship between shear stress and shear rate of a shear thinning fluid as follows:

$$\tau = K\,\gamma^{n} \tag{1.1}$$

τ: Shear Stress (lb/100 ft^2)

K: Consistency Index (lb-s^n/100ft^2)

γ : Shear Rate (s^{-1})

n: Flow Behavior Index

Power law introduces consistency index “K”, which serves as a quantifier for the fluid’s internal resistance to motion, instead of the viscosity term in Newtonian model. To differentiate between Newtonian and non-Newtonian behavior this model raises the shear rate to nth power, naming the constant “n” as flow behavior index, which is an indication of the degree of dependence of fluid’s viscosity to the applied shear stress. Deviation of this number from 1 means increasing non-Newtonian behavior. This model can describe dilatant fluids when $n>1$ and pseudoplastic fluids when $n<1$. If $n=1$ the model reduces to a Newtonian fluid.

Although it is one of the simplest ways, Power Law Model has serious disadvantages: The model can only be applied to a limited range of shear rates and the model constants depend on the considered range. Also Power Law Model fails to predict viscosities at zero and infinite shear rates. Despite the model’s shortcomings it’s widely used in field because of its practicality.

1.1.2 BINGHAM PLASTIC MODEL

Some fluids have a certain limiting stress (yield stress) which is the resistance to flow due to dispersion and the attraction between the solid particles. This kind of fluids behaves visoplastically and the simplest model to define such behavior is Bingham Plastic Model. The model can be expressed mathematically as follows:

$$\tau = \tau_y + \mu_p \gamma \qquad (1.2)$$

τ: Shear Stress (lb/100 ft^2)

τ_y: Yield Stress (lb/100 ft^2)

γ : Shear Rate (s^{-1})

μ_p: Plastic Viscosity (cp)

Bingham Plastic model is characterized by a yield stress (τ_o) term which defines the amount of stress needed to initiate flow and a plastic viscosity (μ_p) term which is not dependent on the shear rate. Since most oilfield fluids exhibit shear rate dependence after initiation of flow, this model has some shortcomings describing them [3].

1.1.3 HERSCHEL-BULKLEY MODEL

More recently, the Herschel-Bulkley model has seen increased usage because it accommodates the existence of a yield point (Bingham plastic) as well as the nonlinearity of the relationship of shear stress to shear rate (Power-law) [4]. Herschel-Bulkley can be used in defining a variety of oilfield fluids accurately. Herschel-Bulkley Model adds a yield stress parameter to Power Law model and thus contains three parameters as follows:

$$\tau = \tau_y + K \gamma^n \qquad (1.3)$$

τ: Shear Stress (lb/100 ft^2)
τ_y: Yield Stress (lb/100 ft^2)
γ : Shear Rate (s^{-1})
K: Consistency Index (lb-s^n/100ft^2)
n: Flow Behavior Index

With the introduction of powerful computational equipment, more complex models like Herschel–Bulkley, which can account for both power law fluids and Bingham plastic fluids, are gaining larger recognition.

The rheological parameters obtained by rheometry are used in evaluating hole cleaning and hole erosion problems, suspension of cuttings, drilling fluid treatment, and hydraulic calculations.

1.2 ABOUT THE POLYMERS USED IN THIS STUDY

In this study, xanthan gum and polyanionic cellulose solutions are used experimentally. There are numerous reasons behind the use of these two polymers:

1- Both polyanionic cellulose and xanthan gum are commonly used in drilling and completion fluid preparation.

2- Polyanionic cellulose and xanthan gum provide high levels of viscosity when compared to many other additives. These high viscosity profiles have provided an ease of investigation in this study.

3- The viscometer used in this study can only make a measurement at a specified shear rate if it completes a full revolution and at low shear rates this proves to be a time consuming process and limited the number of polymers used in this study.

This study is performed in order to determine the rheological characteristics of some commonly used water soluble polymers in formulating drilling and completion fluids, especially under ultra-low shear rate conditions. Experiments were conducted with the use of an OFITE Model 900 Low Shear Rate Viscometer. During experiments effect of the polymer’s concentration, fluid’s temperature and applied shear rate were investigated. Rheograms of different samples were constructed under different concentrations and temperature conditions and rheological behavior of the polymer were discussed and explained with a fitting rheological model.

CHAPTER 2

LITERATURE REVIEW

Drilling fluids, which represent one fifth (15 to 18%) of the total cost of oil well drilling, must generally comply with three important requirements: they should be, i) easy to use, ii) not too expensive and iii) environmentally friendly. The complex drilling fluids play several functions simultaneously. They are intended to clean the well, hold the cuttings in suspension, prevent caving, ensure the tightness of the well wall, flood diesel oil or water and form an impermeable cake near the wellbore area. Moreover, they also have to cool and lubricate the tool, transfer the hydraulic power and carry information about the nature of the drilled formation by raising the cuttings from the bottom to the surface [2].

A fair amount should be known to realize the effect of fluid properties on different drilling and completion operations so one can solve various problems which can be encountered during these operations. Solution of these possible problems is also very important on project economics. The impact of rheology on numerous aspects of the drilling and completion process has been reported. Some of the more important aspects include the management of the equivalent circulating density, control of barite sag and enhanced hole cleaning [5]. A drilling mud is a complex fluid which comprises of multitude of additives. The type and amount of additives is based on the drilling method employed and the type of reservoir to be drilled. The drilling mud can be broadly classified as water based mud (WBM), oil based mud (OBM), synthetic based mud (SBM), emulsions, invert emulsions, air, foam fluids, etc.

Slatter developed a new annular friction factor for Herschel - Bulkley type fluids based on a modified Reynold's Number as a function of all three Herschel-Bulkley viscosity parameters. Slatter's work appears to accurately predict the laminar to turbulent transition [6].

Accurately predicting rheological properties of hydraulic fracturing fluids is essential for designing and executing an optimum treatment. Fluid viscosity affects several important components such as friction loss within well tubulars, leak-off, and fracture geometry and proppant placement [7].

Kenny, Sunde and Hemphill discussed how the Herschel - Bulkley model can be applied to drill cuttings transport analysis when considering other relevant factors such as pumping rate, particle settling velocity and annular eccentricity. They introduced the concept of dimensionless fluid lift factors to evaluate differences in hole cleaning capabilities between drilling fluids of varying properties. The proposed model can provide an effective generalized framework for developing friction prediction equations [8].

Conventional calculations of downhole pressure, which assume constant drilling fluid properties, are both practical and accurate enough for routine wells. Downhole static pressures are easy to calculate from mud weight measured at the surface, while additional pressures caused by circulation can be calculated using established relationships between pump rate and drilling fluid rheological properties. Errors that result from ignoring the variations in drilling fluid rheological properties are relatively small when operating in shallow wells. However in high pressure–high temperature, extended reach and deep-water wells, mud properties do vary with temperature and pressure, affecting the accuracy of both surface measurements and bottom hole estimations of mud weight and viscosity.

Equivalent circulating density (ECD) is often much higher than equivalent mud weight (EMW) in HPHT, extended reach, and deep-water wells due to the small annular clearances between the drill pipe and hole wall. ECD is computed from the dimensions of the annulus and, for a given fluid viscosity, increases with pump rate. The calculation becomes increasingly complicated when changes of viscosity with temperature are considered [9].

Significant mud weight variations greater than 4 ppg have been measured in flow line returns when circulating bottoms up after trips. This phenomenon called barite sag does not occur frequently but once it does, its' remediation can become expensive, especially in highly slanted wells. Sag occurrence can lead to pack off, lost circulation, failure to get logging tools to bottom, stuck pipe and some other problems. The effect of fluid rheology on sag settling is being investigated for some time [10] [11].

Recently researchers have mainly seen that barite sag occurs dynamically at low shear rates. Dye, Hemphill and Mullen conducted an experimental work using a flow loop that would produce barite sag. They concluded this phenomenon is related to low shear rate rheology and average annular velocity. Barite sag estimations using Fann 35 viscometers get considerably more accurate when lower shear rate values are incorporated into the rheological modeling procedures. They also developed a barite sag prevention window for use at the rig site by mud engineers to manage dynamic barite sag using low shear rate measurements [12].

Power, Parks and Seheult investigated solids suspension and transport capabilities in fluids which were viscosified with biological polymers and found that these capabilities can be directly correlated to ultra-low shear rate viscosity measured and suspension and transport capabilities do not correlate well with traditional field viscosity measurement [13].

A number of researchers determined a correlation between solid transport and suspending capabilities as well as pressure drop due to friction. Becker et al. [14] saw that when viscosity values at actual pumping shear rates hole cleaning parameters could be determined more accurately. Also these data are comparable with the frictional pressure drop in the annulus. However a more complete relation of hole cleaning with pressure losses were later developed by Gavinet and Sobey [15] and was completed later by Saasen et al[16].

The literature review shows the wide application of rheological properties of drilling and completion fluid rheology. In general, rheological characterization of drilling and completion fluids has been conducted in laboratory and on site and used in various areas like pressure drop estimations, hole cleaning calculations, particle suspension and transport capability analysis, ECD calculations and barite sag prediction and prevention.

CHAPTER 3

STATEMENT OF THE PROBLEM

Rheological properties of drilling and completion fluids can be used in fluid hydraulics like pressure loss predictions, surge and swab pressure estimations and equivalent circulating density (ECD) calculations; annular hole cleaning modeling; barite sag prevention and particle settling velocity estimation. However to accurately make these predictions one has to know the rheological characteristic behavior of the polymers and the drilling/completion fluid. The main target of this study is to rheologically characterize different water soluble polymers, namely, xanthan gum and polyanionic cellulose which are commonly used in drilling and completion fluids. In this study xanthan gum (KAR-ZAN DS™) and polyanionic cellulose (KAR-PAC R™) provided by Karkim [17] are used. Shear stress–shear rate behavior of the polymers is analyzed experimentally by constructing rheograms.

Experiments are carried using an Ofite Model 900 low shear rate viscometer, under atmospheric pressure with differing concentrations (0.25, 0.5, 0.75, 1.00, 1.25, 1.50 lb/bbl) under different temperatures (60, 100, and 120 °F). Sample fluids are aged at 120 °F for at least two hours. Applied shear stress is measured at several different constant shear rates (0.0017 s^{-1} - 1021.38 s^{-1}). Some of the experiments are performed several times to be sure of reproducibility of the process.

The resulting rheograms are examined in order to determine rheological behavior of the polymer in question. Also effect of differing temperature and concentrations of polymer use is investigated by constructing the appropriate diagrams. The data obtained from the experiments are fitted and analyzed using an appropriate rheological model.

CHAPTER 4

EXPERIMENTAL EQUIPMENT AND MATERIALS

OFITE Model 900 Viscometer, Sterling Multi-Products Model 9bMixer, OFITE Portable Roller Oven Model 174-00 and Avery Berkel Model cc062d10abaaga balance, xanthan gum and polyanionic cellulose were used to prepare the drilling fluid and conduct the necessary experiments. Further detail on each of these equipment types will be given in the following subsections.

4.1 OFITE Model 900 Low Shear Rate Viscometer

4.1.1 General Information

Figure 4.1 -OFITE Model 900 Low Shear Rate Viscometer

Viscometers are used to measure the viscosity of a fluid sample. There are several different viscometers which operate under different principles. Rotational viscometers are one of the most widely used viscometer types. This type of viscometer operates on the principle of measuring the rate of rotation of a solid shape in a viscous medium upon application of a known force or torque required to rotate the solid shape at a definite angular velocity. Rotational viscometers provide several advantages like measurements under steady state conditions, multiple measurements with the same sample at different shear rates, continuous measurement on fluids whose properties may be function of temperature, and small or no variation in the rate of shear within the sample during a measurement [18].

OFITE Model 900 Low Shear Rate Viscometer (Figure 4.1) is a portable and fully automated Couette coaxial cylinder rotational viscometer. While the bob of the viscometer is stationary, the rotor sleeve rotates shearing the sample fluid present between the rotor sleeve and the bob. Internal resistance of the sheared fluid will cause a force on opposite direction which in turn, will induce angular rotation on the bob. The amount of rotation is monitored by a transducer and the processor uses this value to calculate and transmit readable output of the sample characteristics. OFITE Model 900 Low Shear Rate Viscometer is able to operate at both extremely low shear rates with a minimum of 0.001 rotations per minute (0.01 s^{-1}) and the conventionally used industry range of 3 (5.1 s^{-1}) to 600 (1021.4 s^{-1}) rotations per minute. Buttons on viscometer keypad provide easy access to commonly used rotor speeds in oilfield industry as well as some API recommended routines, though specific rotor speeds can also be set.

The viscometer can measure shear stress values at applied respective shear rates. Operating temperatures can be adjusted with the heating cup, whereas a thermocouple connected to the heating cup of the viscometer can measure the current operating temperature.

The viscometer can be operated automatically with the help of a computer. The connection is made from the serial (RS-232) port and the interaction between the user and the viscometer is achieved by the ORCADA ™ software, provided and developed by OFITE. More details about OFITE Model 900 Low Shear Viscometer can be found in Table 4.1.

Table 4.1 - OFITE Model 900 Low Shear Rate Viscometer Specifications

Instrument Geometry	True Couette Coaxial Cylinder
Motor technology	Stepper
Motor Speeds (RPM)	12 Fixed Speeds (600, 300, 200, 100, 60, 30, 20, 10, 6, 3, 2 and 1); Variable speed range 0.006-1000
Speed Accuracy (RPM)	0.001
Shear Rate Range (sec^{-1})	0.01-1700
Readout	Digital
Heat Cup	Stainless Steel, 150 Watts, Maximum Recommended Temp: 190°F (88°C)
Temperature Measurement	Type "J" Thermocouple
Automatic Tests	API Cementing and Mud Rheologies
Power Requirements	97 - 250 Volts AC, 200 Watts, 50/60 Hz
Weight (kg)	8.6
Dimensions (cm)	44 x 38 x 24
Shipping Weight (kg)	16
Shipping Dimensions (cm)	56 x 38 x 24
Computer Requirements	DB-9 Serial Port, Windows 2000 or XP. Recommended screen resolution 1024 x 768 pixels

4.1.2 UNIVERSAL HEAT CUP FOR MODEL 900 VISCOMETER

Universal Heat Cup for Model 900 Viscometer is designed to control the liquid sample temperature while working with OFITE Model 900 Low Shear Rate Viscometer. The Universal heat cup can be used both automatically from within the ORCADA^{TM} software and manually from the knob in front of the heat cup. Desired operating temperature can be set up to 200 ^{o}F (93 ^{o}C). There is also a red pilot light on the heat cup to indicate the current condition of the temperature; when the adjusted temperature value is reached, the pilot light turns on.

Figure 4.2 - Universal Heat Cup for Model 900 Viscometer

4.1.3 ORCADATM MODEL 900 SOFTWARE

The OFITE Model 900 Viscometer is optimized for use with a computer using the ORCADA^{TM} software. When software management is initiated the buttons on the face of the machine are locked and all operation management is continued using the software interface. ORCADA^{TM} Model

900 Software enables the user to automate tests with specific conditions, perform routine tests with ease, and monitor measurements in real time and store results of the measurements for later use. The connection from the viscometer to the computer is made from the serial port (RS-232). The main interface of the program can be seen in Figure 4.3 below.

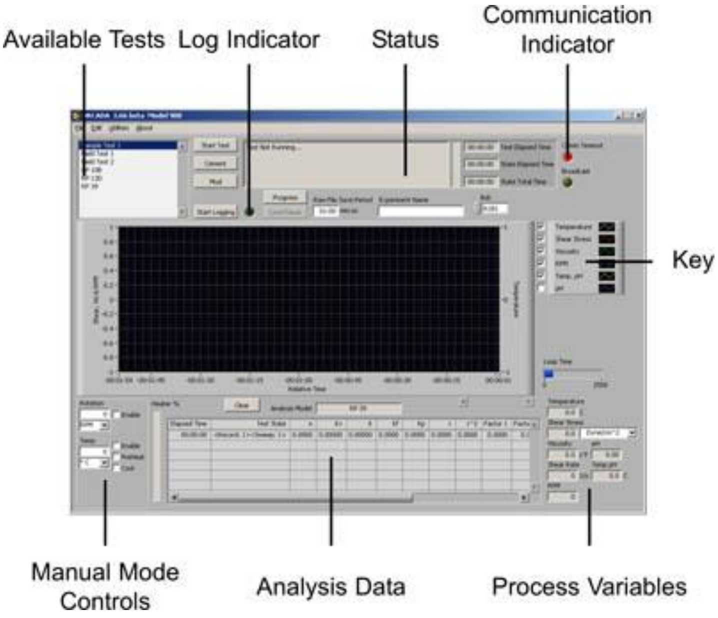

Figure 4.3- Orcada^{TM} Software Home Screen

4.2 STERLING MULTI-PRODUCTS MODEL #9B5 MIXER

Majority of drilling fluids include solid particles in their formulation which needs to be dissolved or mechanically dissipated in the liquid to form a homogeneous mixture. These homogeneous mixtures can be obtained by shearing the fluid and additives mix for an appropriate time, and multi-mixers offer this functionality.

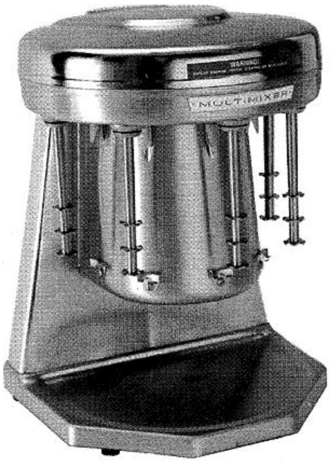

Figure 4.4 - Sterling Multi-Products Model #9B5 Mixer

A Sterling Multi-Products Model #9B5 Mixer is used in this study. The multi-mixer has five spindles and placing a mixing cup on any of these will automatically start the motor. The rotating motion of the spindle will help mix the additives and distilled water homogeneously. The motor will stop after the last mixing cup is removed from its position on a spindle. The multi-mixer and mixing cups conform to American Petroleum Institute (API) Specification 13A for mixing water and oil based drilling fluids.

4.3 OFITE PORTABLE ROLLER OVEN MODEL 174-00 AND OFITE AGING CELL MODEL 175-50

4.3.1 OFITE PORTABLE ROLLER OVEN MODEL 174-00

Drilling fluids undergo the effect of temperature while they are being circulated throughout the wellbore by pumping. Many important fluid properties like viscosity and density change during this circulation. To simulate this phenomenon in laboratory conditions, one can use a roller oven, which is capable of providing both rolling and heating functions for aging cells which contain drilling fluid samples. Aging the drilling fluid in specifically crafted aging cells using a roller oven can provide insight on the behavior of many different additives under varying temperatures.

OFITE Roller Ovens are designed to provide heating and rolling functions simultaneously and independently; meaning that they can be used to age the drilling fluid dynamically or statically. The specific portable roller oven used in this study, OFITE Portable Roller Oven Model 174-00, has three rollers and is capable of holding two 500 ml or four 260 ml aging cells. Rotation speed of the roller oven is factory set to 25 rpm but can be adjusted by the user.

Figure 4.5 - Ofite Portable Roller Oven Model 174-00

Temperature can be set between 38 to 232^{o}C, and can be controlled from the digital indicator present on the top side of the portable roller oven.

4.3.2 OFITE AGING CELL MODEL 175-50

The OFITE Aging Cell is a closed vessel that enables fluid samples to be subjected to high temperatures and maintained in liquid state at the same time. These cells can be used to simulate static and, with the help of a roller oven, dynamic aging conditions. This aging process allows the previously sheared drilling fluid to fully develop rheological and filtration properties.

Figure 4.6 - Ofite Aging Cell Model 175-50

OFITE Aging Cell Model 175-50 comes in 500 ml size, is manufactured from grade 303 (or grade 316) stainless steel and utilizes both Viton® and Teflon® o-ring seals. These aging cells can be used in temperatures as high as 450 ^{o}F.

4.4 NUVE NS 108 WATER DISTILLER

Table 4.2 - NUVE NS 108 Water Distiller Technical Specifications

Distilled Water Capacity	8 liters/hour
Cooling Water Use	80 liters/hour
Water Entry Manometer	0 - 4 kg/cm^2
Power Rate	230 V, 50 Hz, 3 phases
Installed Water	3 x 2000 W
Boiler Volume	6 liters
Inner Surface	Stainless Steel Tinplate
Outer Surface	Electrostatic Powder Coated Aluminum
Outside Measurements	600 x 260 x 830 mm
Package Measurements	750 x 350 x 920 mm
Net Weight	28 kg
Package Weight	38 kg

Nuve NS 108 Water Distiller is ideal for producing distilled water which might be needed in a laboratory environment. Water evaporated by stainless steel heaters in the boiler is condensed in the condenser part which is kept cool with water coming from city grid. Heated water in the condenser part is returned back to the boiler, easing the evaporation process and saving energy.

Figure 4.7 - NUVE Water Distiller

Distilled water is used in the experiments so that any chemical reaction which might occur between polymers used in investigation and any ion/cations is prevented.

4.5 POLYANIONIC CELLULOSE

According to API definition, a PAC ($(C_6H_7O_2(OH)_2CH_2COONa)_n$) is an off-white water soluble polymer only produced from cellulose chemically reacted with carboxy-methyl (anionic) groups. PAC can be categorized based on the degree of substitution, degree of polymerization and the extent of the purification process. The degree of substitution, the mean number of anionic group per cellulose unit, strongly influences the solubility in water, the salt tolerance, the fluid loss control capabilities and inhibition properties of the polymer. The degree of polymerization is the mean number of glucose units linked together to form the polymer chain. The high viscosity PAC used in this research has high degree of polymerization (high molecular weight) [19].

PAC is an effective additive for reducing the API filtration rate of many water based drilling fluids and can also be used to increase viscosity and improve wellbore cleaning and suspension capabilities in a wide variety of fluid environments. It also coats and encapsulates the cuttings and drilling fluid solids, thereby inhibiting the swelling and disintegration of water sensitive solid particles.

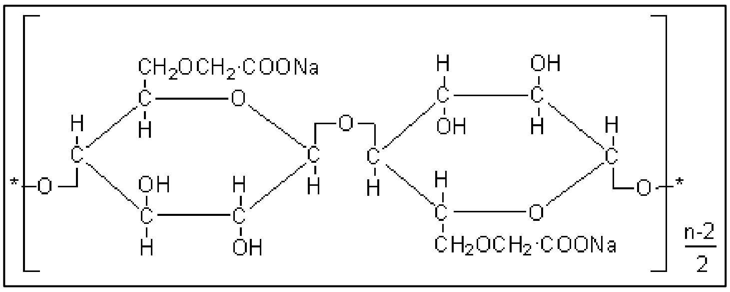

Figure 4.8 – Chemical Structure of Polyanionic Cellulose

4.6 XANTHAN GUM

The API xanthan gum ($(C_{35}H_{49}O_{29})_n$) is defined as "a high molecular weight water soluble biopolysaccharide, commercially produced by a distinct fermentation process of Xanthomonas campestris." Xanthan gum is used as a viscosifier and suspending agent in various drilling and completion fluids [19]. Water solutions of xanthan gum are more pseudoplastic than other polysaccharide products, when shear rate is applied viscosity is reduced in proportion to the amount of shear. Upon the release of shear total viscosity recovery occurs almost instantaneously [20].

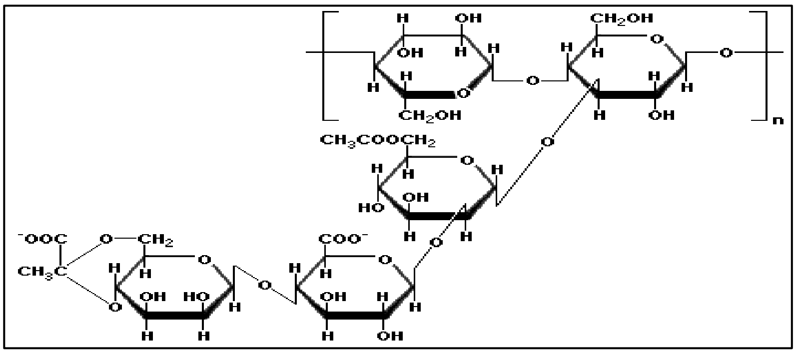

Figure 4.9 - Chemical Structure of Xanthan Gum

CHAPTER 5

EXPERIMENTAL PROCEDURE

To simulate the behavior of drilling mud under real world conditions as much as possible and to get accurate, consistent and repeatable results, one needs to define the methodology that is going to be used very carefully. The subsections of this chapter will explain the experimental procedure used in this study in detail.

5.1 Preparation of the Drilling Fluid

1. At high pH values (pH>10) xanthan gum tends to form gels in the presence of high concentrations of divalent cations. Trivalent cations such as aluminum or iron form gels at acid or neutral pH levels. To prevent such gelation, all samples are prepared by using the distilled water produced by using a NUVE NS 108 water distiller.

2. 350 milliliters of distilled water, measured by the help of graduated cylinder, is poured into a clean mixer cup.

3. Varying quantities (0.25, 0.50, 0.75, 1.00, 1.25 and 1.50 grams) of the water soluble polymer in question is added into the mixer cup while the mixer cup is in place on one of the spindles of the multi-mixer.

4. The drilling fluid sample is then mixed for 10 minutes allowing for the polymers to dissolve homogeneously in water.

5. Drilling fluid sample is then carefully poured to a clean aging cell, leaving about one and a half inch from the top of the cell for fluid expansion. An o-ring is placed in the groove of the aging cell body, after checking it for any defects. Inner cup is placed above the aging cell so that the o-ring seats in place, followed by the outer cup which is hand tightened. The center set screws in middle of the outer cup are tightened using an Allen wrench.

6. The aging cell is placed in the portable roller oven. After digital temperature control of the roller oven is adjusted to 48.9 $^{\circ}$C (120 $^{\circ}$F), the heater and rollers are switched on.

7. The drilling mud sample is allowed to age for at least for two hours under dynamic conditions at 48.9 $^{\circ}$C (120 $^{\circ}$F).

8. After the aging process is completed, the aging cell is taken out of the portable roller oven. Outer cup center set screws are loosened with the help of an Allen wrench and the inner cup is removed.

9. The drilling fluid sample is poured into a clean mixer cup and placed on one of the spindles of the multi-mixer. The fluid is sheared for 10 minutes allowing any settled polymer to solve in water.

10. Approximately 170 milliliters of the drilling fluid is separated with the help of a graduated cylinder, then transferred to the viscometer's sample cup and the sample cup is placed inside the universal heat cup

available for the viscometer. The thermocouple connected to the viscometer is placed inside the hole present.

11. The rotor sleeve is immersed in the sample to mark on the sleeve by moving up the stand. Once the stand is in place, the lock nut present on it is tightened.

12. A thin film is used to cover the openings of the viscometer's sample cup so that loss of sample to the atmosphere is minimized.

13. The viscometer is operated from a personal computer which has ORCADA ^{TM} software installed and configured. A new test is created with a fitting name and a previously prepared test configuration is used. Once the viscometric measurements are done, obtained data is tabulated in a fitting way.

Details of the test and software configuration will be explained in the following subsections in details.

5.2 OPERATION OF THE VISCOMETER VIA ORCADA TM

5.2.1 TEST BUILDER

1. The test builder can be accessed from the edit menu on the starting screen of ORCADA software. A new test procedure is created by pressing the new test button.
2. After naming the new test procedure, one can start to define the actions that the viscometer and the heat cup will follow, by filling each required line in record field.

5.2.2 TESTS

Various drilling fluid samples prepared as stated in the previous section are evaluated using different testing procedures to analyze their rheological characteristics. Each of these fluids was tested to construct their rheograms. Thixotropic behavior tendency, effect of temperature and concentration on apparent viscosity were tested and yield stress evaluation has been made. All tests are repeated several times to make certain the results obtained are reproducible in an acceptable range.

Prepared fluid samples are first heated or cooled to the test temperature and during the tests temperature stays constant with a threshold of ± 1^{o}F. Then the samples are sheared at 600 rotations per minute (1021.38 s^{-1}) for twenty seconds and respective apparent viscosity and shear stress values are measured. Shear rates are lowered in 22 steps from 600 rotations per minute (1021.38 s^{-1}) to 0.01 rotations per minute (0.017 s^{-1}). At each speed the viscometer takes several readings during the shear period and records the average as a result. Viscometer needs to finish one full rotation to give a measurement at each constant shear rate, so the viscometer shears for either 20 seconds or the time it takes for one full rotation, which takes longer. At lower shear rates this process proves to be a time limiting factor. After the measurement at 0.017 s^{-1} , a similar sweep is performed backwards from 0.017 s^{-1} to 1021.38 s^{-1}. Similar measurements are conducted with different concentration of polymers at different temperatures.

Table 5.1 – Hysteresis loop construction.

Mode	From	To
Down – sweep	1021.38 s^{-1}	0.017 s^{-1}
Up – sweep	0.017 s^{-1}	1021.38 s^{-1}

Test temperatures were selected as 60°F, 100°F and 120°F. The limitation behind the selection of this temperature range was the capabilities of the available experimental equipment; neither the viscometer nor the heating cup available have any cooling capabilities so the lower limit was selected as room temperature (60°F) and after the upper limit 120°F, covering the sample cup with a thin film was not enough to prevent the effect of vaporization of the fluid sample.

CHAPTER 6

RESULTS, DISCUSSION AND ANALYSIS

Viscometric analysis has been used as a tool for the characterization of the rheological behavior of different polymers commonly used in drilling and completion fluids. Rheological analysis has been frequently applied to study drilling and completion fluids flow behavior. However works including low end rheology (ultra-low shear rate rheology) are not very common until recent years. The data obtained from the conducted experiments will be presented and analyzed in the following subsections.

6.1 XANTHAN GUM

6.1.1 XANTHAN GUM RHEOLOGY

Oilfield standard Fann Model 35 viscometer has six speeds varying from 3 rpm (5.107 s^{-1}) to 600 rpm (1021.38 s^{-1}). General viscosity readings at field are made using this range so investigating the rheograms constructed in two pieces, a traditional shear rate range and a low shear rate range can give some invaluable insight. Numeric results for XCD solution experiments can be found in Appendix C.

It can be seen from Figure 6.1 that the xanthan gum is showing shear thinning effects; the increase in shear rate is causing a decrease in viscosity. According to J.W. Powell, "the low apparent viscosity of xanthan gum when measured at high shear rates in a coaxial cylinder viscometer can be explained by combination of a minute depletion layer at the wall of the pipe containing less polymer than the bulk fluid, wall slip effects attributed to the depletion layer and lining up of polymer molecules in regions of high velocity gradient at the pipe wall".

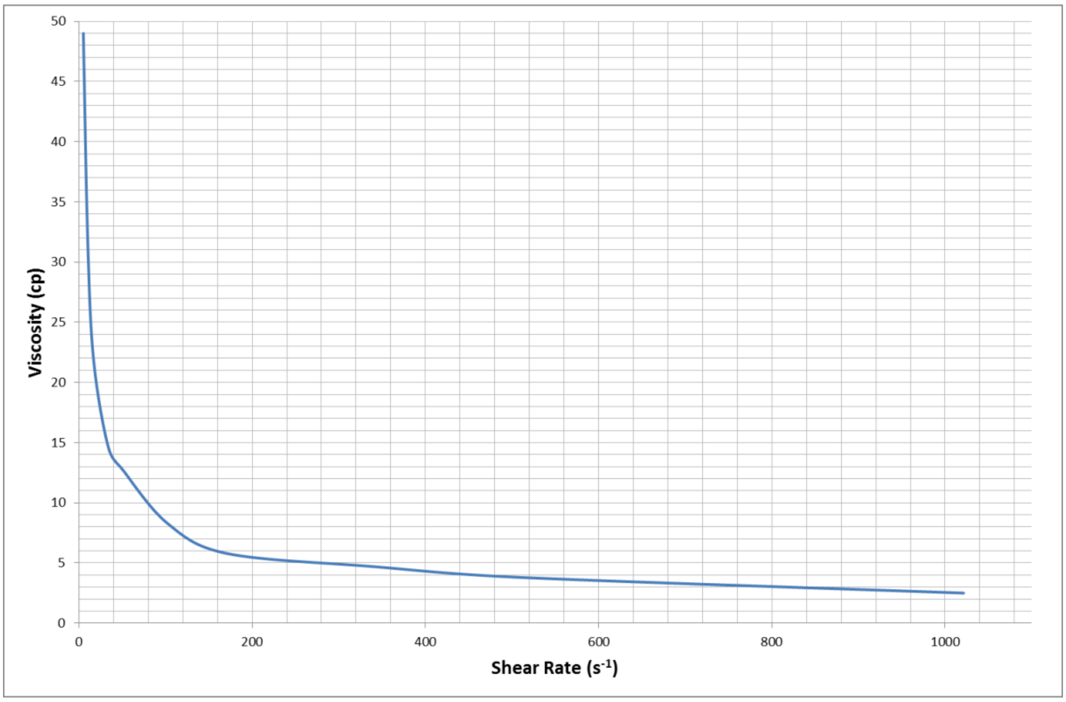

Figure 6.1 – Viscosity – Shear Rate Graphic of 0.25 lb/bbl XCD Solution @ 60 ˚F

These happenings lower the flow behavior index ("n") value which causes a flatter shear stress – shear rate relation as can be seen in Figure 6.2. As Powell states, "the shear thinning of xanthan results in increased shear stress and shear rate at the pipe wall, improving solids transport in horizontal wells by increasing cuttings bed erosion; lower pump pressures and increased pump rates" [13]. It is seen that the increase in viscosity with the decrease of applied shear rates is much more pronounced within the lower shear rate region.

The flow curves obtained by increasing and decreasing the applied shear rate are one of the techniques to analyze thixotropy. The area between these curves is called the hysteresis area and gives information about the time-dependent behavior of the fluid, in terms of different durations of break-down and build-up of the structural network. It is evident from Figure 6.2 that xanthan gum is highly pseudoplastic, there is not any noticeable hysteresis; even after high shear rates the initial viscosity is quickly rebuilt independent of time. This behavior results from the ability of xanthan molecules, in solution to form aggregates through hydrogen bonding and polymer entanglement.

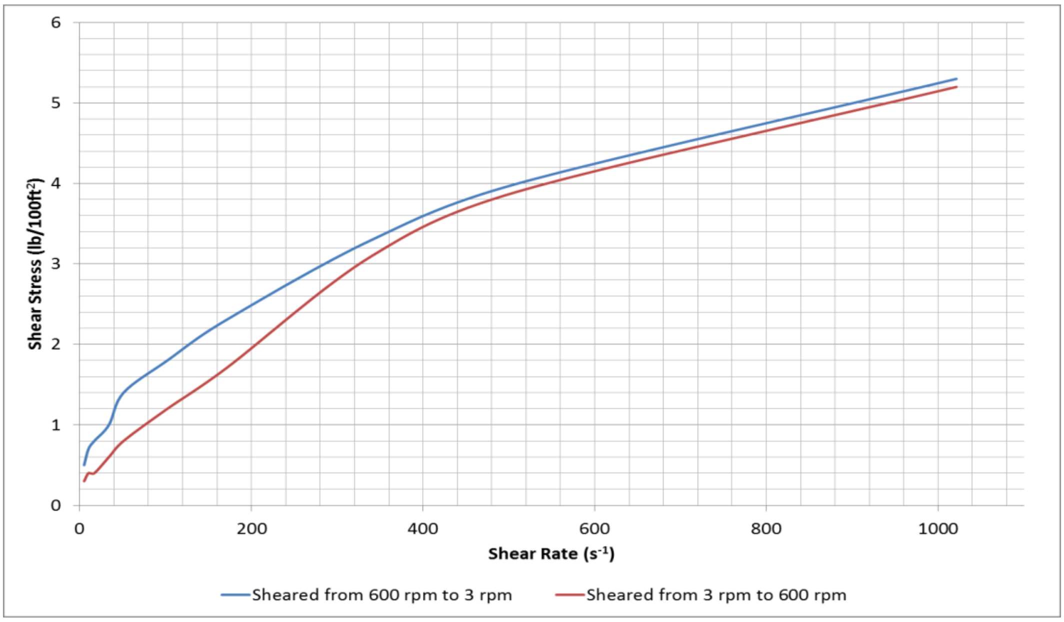

Figure 6.2- Shear Stress – Shear Rate Graphic of 0.25 lb/bbl XCD Solution @ 60 ˚F

This highly ordered network of entangled, stiff molecules results in high viscosity at low shear rates, and in practical terms, accounts for the outstanding suspending properties of xanthan gum solutions. These aggregates are progressively disrupted under the influence of applied shear, hence the highly pseudoplastic flow characteristics of xanthan gum solutions. Pseudoplasticity of xanthan gum enhances mixing and pumping properties of the drilling or completion fluid with xanthan gum in it [21].

Figure 6.3 presents change of measured apparent viscosity values at constant shear with the effect of concentration. It is obvious that introducing more xanthan gum to the drilling or completion fluid will increase measured viscosity values. This behavior is attributed to the intermolecular interaction or entanglement, increasing the effective macromolecule dimensions and molecular weight [22]. The effect of polymer concentration on apparent viscosity values become more pronounced at lower shear rates. While a more flat and linear increase in viscosity is seen with increasing concentrations at higher shear rates, the rate of increase gets bigger as the shear rate is lowered.

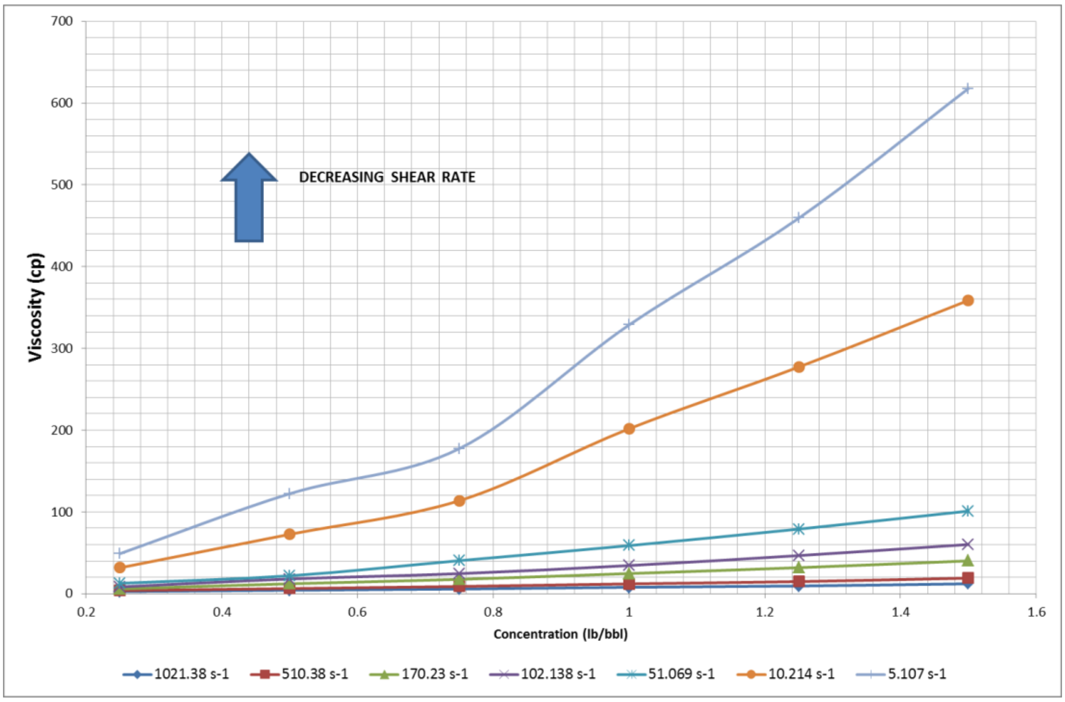

Figure 6.3-Effect of Concentration on Apparent viscosity of XCD Solution @ 60 ˚F

Effect of changing the ambient temperature with other parameters kept constant can be seen in Figure 6.4. As temperature increases the average speed of molecules increase decreasing the amount of time they spend in contact with the nearest neighboring molecule which also results in the decrease of average intermolecular forces. The figure shows results as expected, the increase in temperature results in the decrease of measured viscosity values.

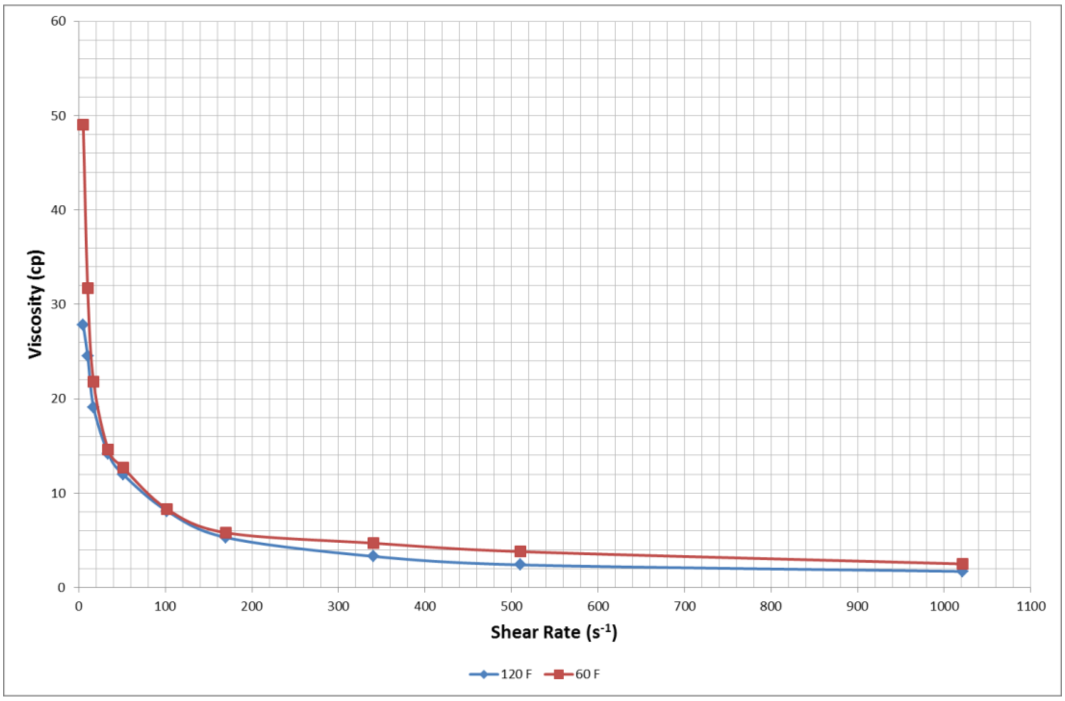

Figure 6.4-Effect of Temperature on Apparent Viscosity of 0.25 lb/bbl XCD Solution

6.1.2 MATHEMATICAL MODELING OF XANTHAN GUM RHEOLOGY

To present the experimental data obtained in a conventional mathematical way, one needs to use a rheological model. The low-to-ultra low shear rate data should be fit by a rheological model that is capable of incorporating them in the calculation procedure. The Herschel-Bulkley rheological model has been shown to handle low shear rate data well [23]. Flow parameters of power law and Bingham plastic rheological model, since they are the most widely used rheological model in oilfield because of its practical use, are also computed for some concentrations to compare their respective accuracies.

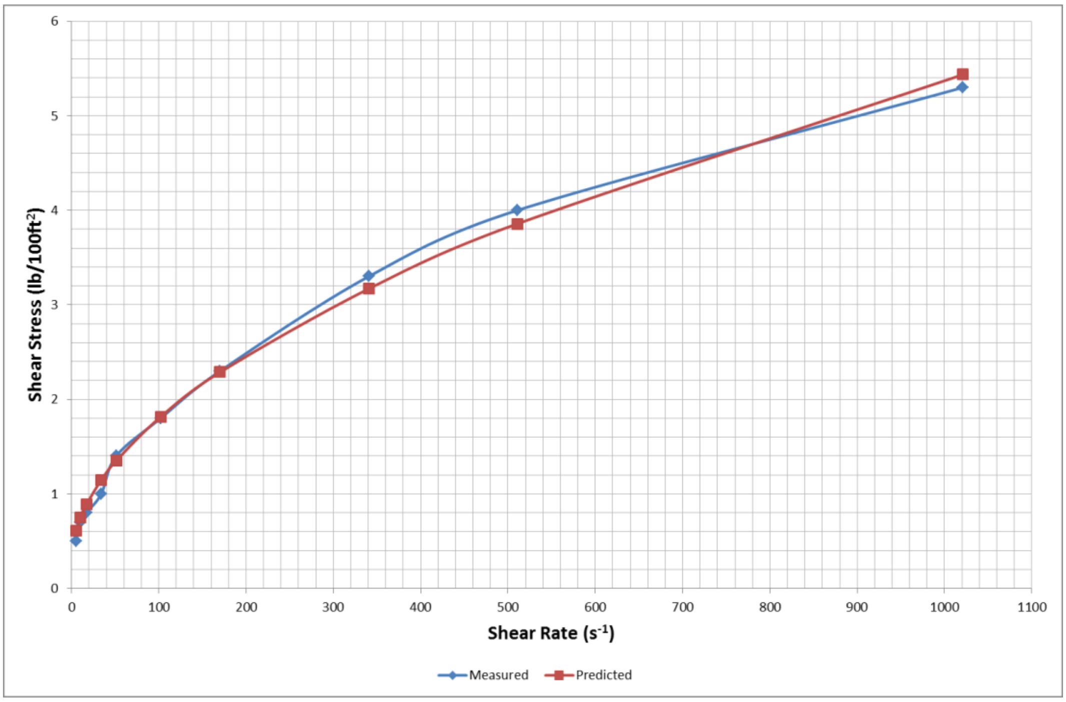

Figure 6.5 – Measured and Hershel – Bulkley Model Predicted Values for 0.25 lb/bbl XCD Solution @60 ˚F (without inclusion of low shear rate values)

Yield stress of an aqueous solution is generally defined as a critical applied stress value below which the liquid shows resistance to flow. When the applied critical stress exceeds this limit, viscous deformation is observed and the liquid starts to flow. There are various definitions of this critical parameter according to different points of view. In this study the stress measurement when shear rate is 0.017 s^{-1}, is accepted as a reading for the yield stress since it is a good estimation of zero shear rate stress. The remaining Herschel – Bulkley parameters, flow behavior index and consistency index are then found using a curve fitting method while using least squares method to find the best match. It can be seen that Herschel –Bulkley model is well suited to describing both low shear rate rheology and the traditional range of Fann viscometer shear rates fairly accurately.

It can be observed that the inclusion of low shear rate measurements tend to change the model parameters noticeably. However this does not noticeably affect the ability of the model to predict stress values accurately.

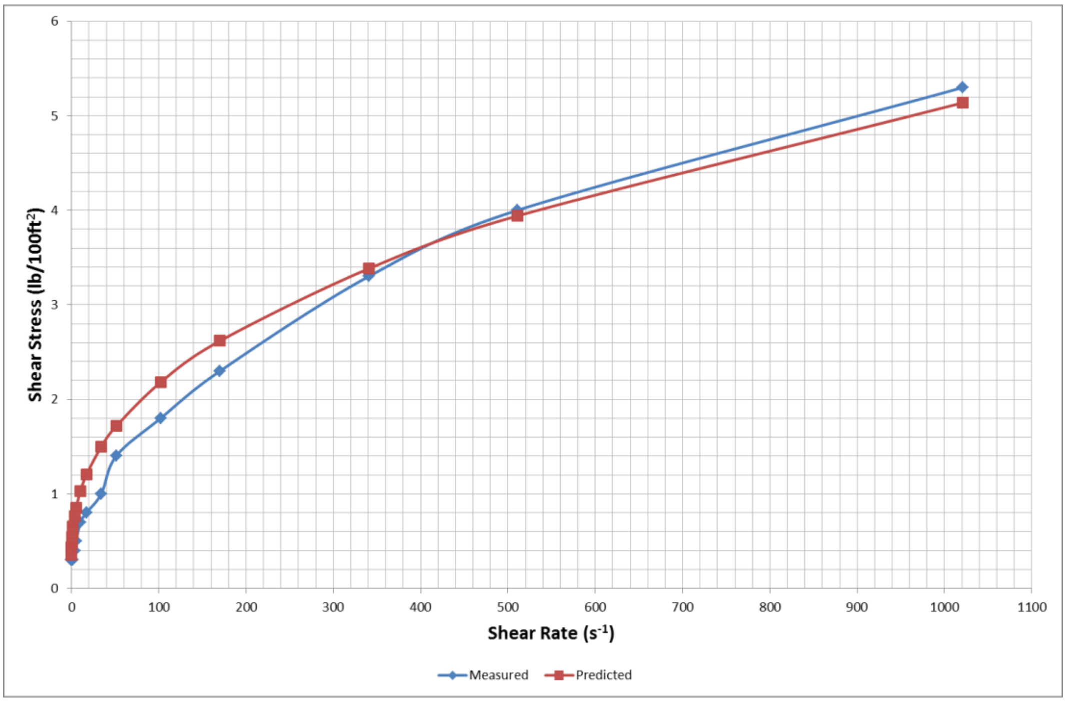

Figure 6.6 – Measured and Hershel–Bulkley Model Predicted Values for 0.25 lb/bbl XCD Solution @60 °F (with inclusion of low shear rate values)

Table 6.1 – Computed Herschel–Bulkley Rheological Model Parameters for Xanthan Gum at 60 °F (without inclusion of low shear rate parameters)

Concentration (lb/bbl)	τ_y (lb/100ft^2)	K (lb-s^n/100ft^2)	n (-)
0.25	0.300	0.131	0.530
0.50	0.400	0.353	0.460
0.75	0.500	0.804	0.383
1.00	0.600	1.494	0.337
1.25	0.800	2.306	0.302
1.50	1.000	3.082	0.296

Table 6.2 – Computed Herschel–Bulkley Rheological model parameters for Xanthan Gum at 60 °F (with inclusion of low shear rate parameters)

Concentration (lb/bbl)	τ_y (lb/100ft^2)	K (lb-s^n/100ft^2)	n (-)
0.25	0.282	0.152	0.511
0.50	0.418	0.357	0.458
0.75	0.452	0.765	0.393
1.00	0.600	1.390	0.349
1.25	0.800	2.249	0.306
1.50	0.950	3.229	0.288

The effect of concentration on computed Herschel–Bulkley model parameters were defined mathematically as follows:

$$\begin{aligned} \tau_y &= 0.6055\ C + 0.0252 && \text{(a)} \\ K &= 1.4296\ C^{1.7358} && \text{(b)} \\ n &= -0.1842\ C + 0.5455 && \text{(c)} \end{aligned} \tag{6.1}$$

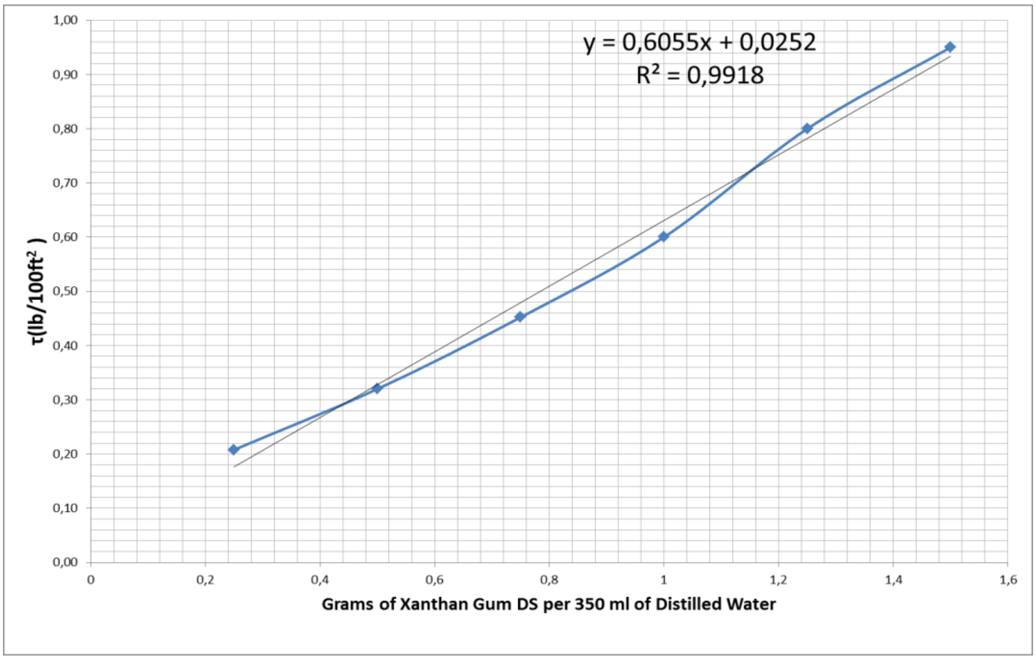

Figure 6.7 – Effect of Concentration of Xanthan Gum on Yield Stress @ 60°F

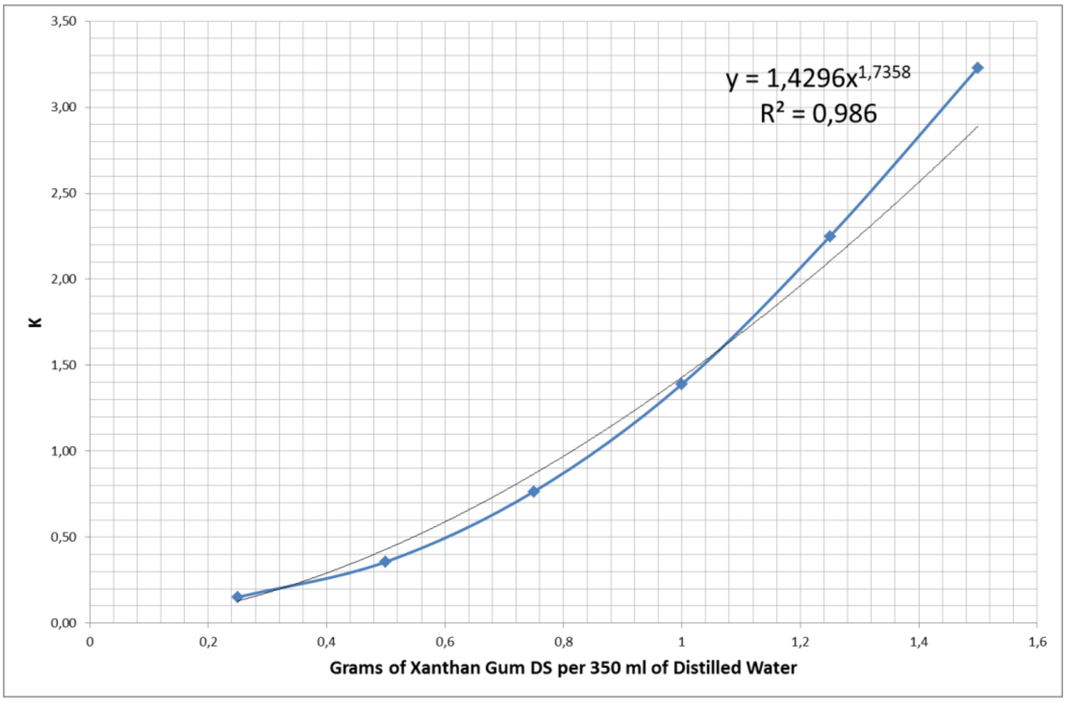

Figure 6.8 – Effect of Concentration of Xanthan Gum on K @ 60°F

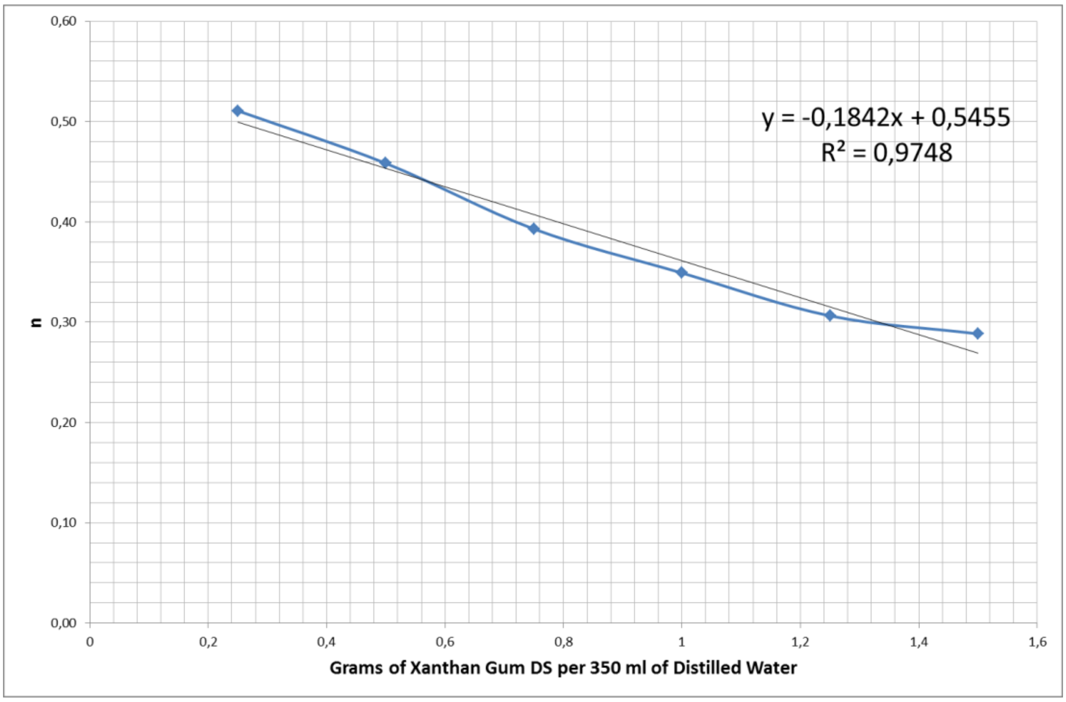

Figure 6.9 – Effect of Concentration of Xanthan Gum on n @ 60°F

The combined effect of shear rate and concentration on shear stress becomes at 60°F:

$$\tau = (0.6055\ \mathrm{C} + 0.0252) + (1.4296\ \mathrm{C}^{1.7358})\ \Upsilon^{(-0.1842\ \mathrm{C} + 0.5455)} \qquad (6.2)$$

The effect of ambient temperature is one of the most pronounced effects on apparent viscosity of fluids. Previous experimental work show that apparent viscosity of most fluids decrease with increasing temperature, not significantly dependent on pressures up to several atmospheres. The result is not different for this case; with increasing ambient temperature the measured apparent viscosity values of xanthan gum solution are decreasing. The effect of operating temperature on xanthan gum rheology can be seen below:

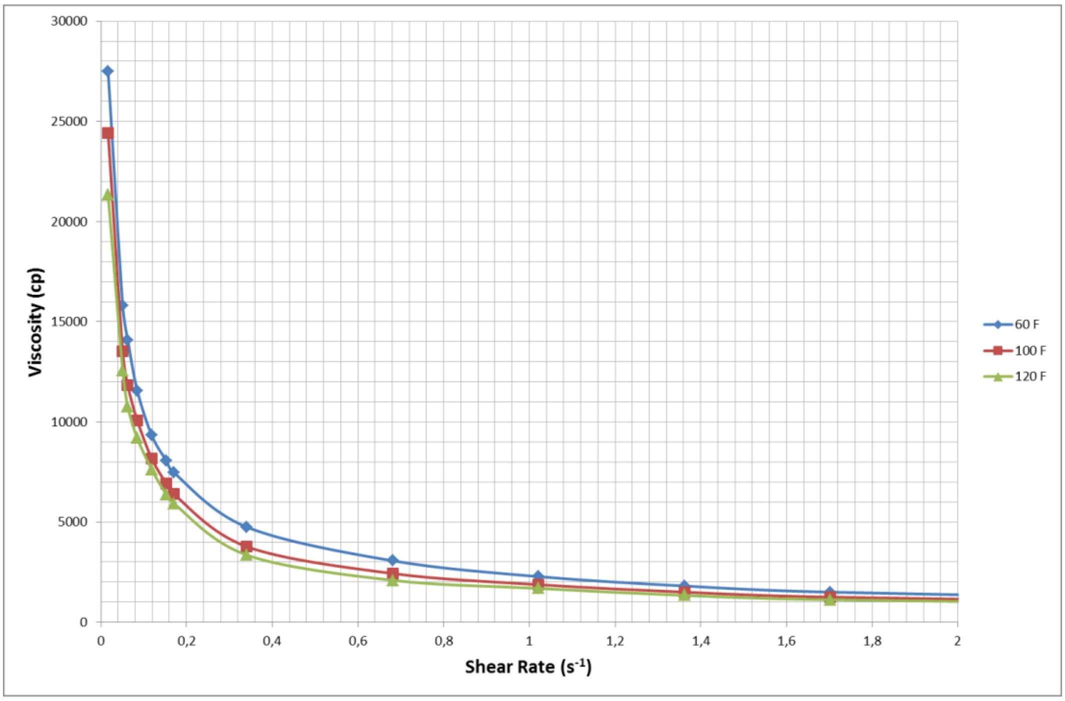

Figure 6.10 – Effect of Temperature on 1.5 lb/bbl XCD Solution

As already mentioned earlier, power law, Bingham plastic and Herschel – Bulkley models are compared for their respective accuracies in representing the shear rheology of xanthan gum. It can be seen from Table 6.4 that while Herschel–Bulkley model can do a comparatively accurate representation overall the shear rate range, Bingham plastic model produces lower shear stress values at higher shear rates and power law model produces lower shear stress values at lower shear rates. In Bingham plastic model the lower shear stress predictions at higher shear rates are caused by an assumption of constant plastic viscosity while the fluid sample shows shear thinning characteristics and the lower shear stress predictions at lower shear rates in the case of power law is caused by a lack of yield stress representation in the model. Since the viscometer is only capable of measuring shear stress values with a minimum accuracy of 0.1 lb/100 ft^2, this situation adds to the difference between the measured results and the rheological model predictions, especially at low shear stress values. This limitation also holds for other concentrations, temperatures and PAC solution experiment results. Similar results are obtained when checked at different concentrations and temperatures.

Table 6.3– Measured and Predicted Shear Stress Values for 0.25 lb/bbl XCD Solution @ 60 °F

Shear Rate (s^{-1})	Shear Stress (lb/100 ft^2)	Bingham Shear Stress (lb/100 ft^2)	Power Law Shear Stress (lb/100 ft^2)	Herschel- Bulkley Shear Stress (lb/100 ft^2)
1021.38	5.3	5.91759	5.244266	5.524499
510.69	4	3.108795	3.944593	3.960849
340.46	3.3	2.17253	3.339278	3.272401
170.23	2.3	1.236265	2.511714	2.380471
102.138	2	0.861759	2.0362	1.898361
51.069	1.6	0.58088	1.531574	1.416258
34.046	1.3	0.487253	1.296547	1.203997
17.023	0.8	0.393627	0.975227	0.928998
10.214	0.7	0.356177	0.790605	0.780359
5.107	0.5	0.328089	0.594671	0.631717
3.405	0.4	0.318728	0.503437	0.566286
1.702	0.4	0.309361	0.378626	0.481464
1.362	0.3	0.307491	0.345498	0.459995
1.021	0.3	0.305616	0.30692	0.435623
0.681	0.3	0.303746	0.259874	0.406906
0.34	0.3	0.30187	0.195352	0.369585
0.17	0.3	0.300935	0.146939	0.343461
0.153	0.3	0.300842	0.140714	0.34024
0.119	0.3	0.300655	0.126909	0.333221
0.085	0.3	0.300468	0.110523	0.32513
0.063	0.3	0.300347	0.097726	0.319009
0.051	0.3	0.300281	0.089599	0.315221
0.017	0.3	0.300094	0.057052	0.30095
Mean Square Error		0.313681	0.017778	0.011514

Table 6.4 – Measured and Predicted Shear Stress Values for 0.50 lb/bbl XCD Solution @ 100 °F

Shear Rate (s^{-1})	Shear Stress (lb/100 ft^2)	Bingham Shear Stress (lb/100 ft^2)	Power Law Shear Stress (lb/100 ft^2)	Herschel- Bulkley Shear Stress (lb/100 ft^2)
1021.38	9	9.734559	9.736668	10.13763
510.69	6.6	5.048367	7.503315	7.524521
340.46	5.4	3.486303	6.44259	6.33386
170.23	4.3	1.924239	4.964818	4.739904
102.138	3.5	1.299413	4.097419	3.8456
51.069	2.5	0.830794	3.157571	2.918328
34.046	2.1	0.674588	2.711193	2.495817
17.023	1.6	0.518381	2.089312	1.930195
10.214	1.4	0.455901	1.724303	1.612858
5.107	1.2	0.409038	1.32879	1.283809
3.405	1.1	0.39342	1.140984	1.133911
1.702	0.9	0.377793	0.879173	0.933114
1.362	0.9	0.374673	0.808526	0.880796
1.021	0.9	0.371544	0.72552	0.820473
0.681	0.8	0.368424	0.62307	0.747889
0.34	0.7	0.365295	0.479888	0.650417
0.17	0.6	0.363735	0.369813	0.579236
0.153	0.6	0.363579	0.355453	0.570232
0.119	0.5	0.363267	0.323411	0.5504
0.085	0.5	0.362955	0.284987	0.527127
0.063	0.5	0.362753	0.254641	0.509176
0.051	0.4	0.362643	0.235197	0.497891
0.017	0.4	0.362331	0.155626	0.453764
Mean Square Error		1.199882	0.221348	0.175376

Herschel-Bulkley model for xanthan gum solutions at 100 °F as a function of concentration and shear rate become:

$$\tau = (0.6629\ C + 0.0533) + (1.3722\ C^{1.6685})\ \Upsilon^{(-0.1797\ C + 0.5398)} \qquad (6.3)$$

Table 6.5 – Measured and Predicted Shear Stress Values for 0.50 lb/bbl XCD Solution @ 120 °F

Shear Rate (s^{-1})	Shear Stress (lb/100 ft^2)	Bingham Shear Stress (lb/100 ft^2)	Power Law Shear Stress (lb/100 ft^2)	Herschel- Bulkley Shear Stress (lb/100 ft^2)
1021.38	7.1	7.445027	6.15393	6.051558
510.69	5	3.848327	4.777921	4.578682
340.46	4.1	2.649426	4.120441	3.897214
170.23	2.7	1.450526	3.199117	2.971428
102.138	1.8	0.970966	2.654774	2.443284
51.069	1.5	0.611296	2.061171	1.886719
34.046	1.3	0.491406	1.777537	1.629208
17.023	1.1	0.371516	1.380083	1.279376
10.214	0.8	0.323562	1.145264	1.079809
5.107	0.6	0.287594	0.889185	0.869495
3.405	0.4	0.275607	0.766853	0.772208
1.702	0.4	0.263613	0.595322	0.63996
1.362	0.3	0.261218	0.5488	0.605053
1.021	0.3	0.258817	0.49399	0.564525
0.681	0.3	0.256422	0.42609	0.515301
0.34	0.3	0.254021	0.330639	0.44822
0.17	0.3	0.252823	0.256709	0.398295
0.153	0.3	0.252704	0.247021	0.391907
0.119	0.3	0.252464	0.225363	0.377771
0.085	0.3	0.252225	0.199309	0.361049
0.063	0.3	0.25207	0.178662	0.348038
0.051	0.2	0.251985	0.165396	0.339801
0.017	0.2	0.251746	0.110743	0.307049
Mean Square Error		0.370678	0.140098	0.12432

Herschel-Bulkley model for xanthan gum solutions at 100 °F as a function of concentration and shear rate become:

$$\tau = 0.1328\, e^{1.2782C} + 0.0988 e^{2.288C}\, \Upsilon^{(-0.1373C+0.4913)} \qquad (6.4)$$

6.2 POLYANIONIC CELLULOSE

6.2.1 RHEOLOGY OF POLYANIONIC CELLULOSE

PAC is showing shear thinning characteristics like xanthan gum; increasing shear rates cause a decrease in apparent viscosity values. Just like xanthan gum, the shear thinning attribute helps with hole cleaning and friction pressure losses. It can be seen that the rate of change of viscosity is much higher at lower shear rate values. Numeric results for PAC solution experiments can be found in Appendix D.

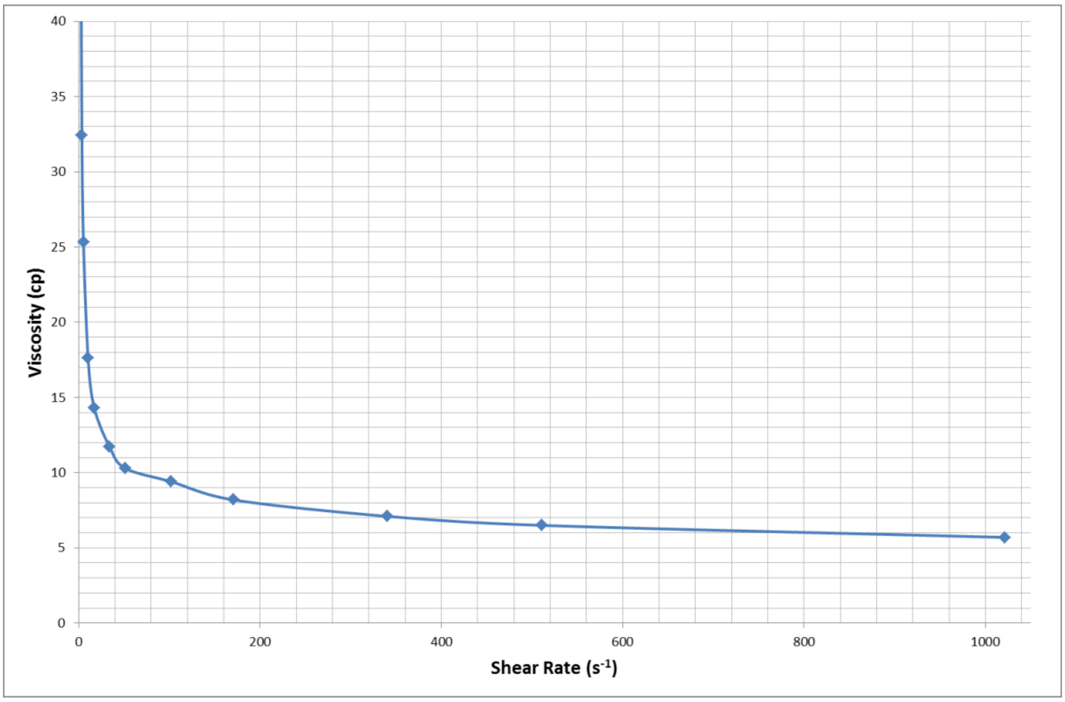

Figure 6.11 - Viscosity - Shear Rate Graphic of 0.25 lb/bbl PAC Solution @ 60 ˚F

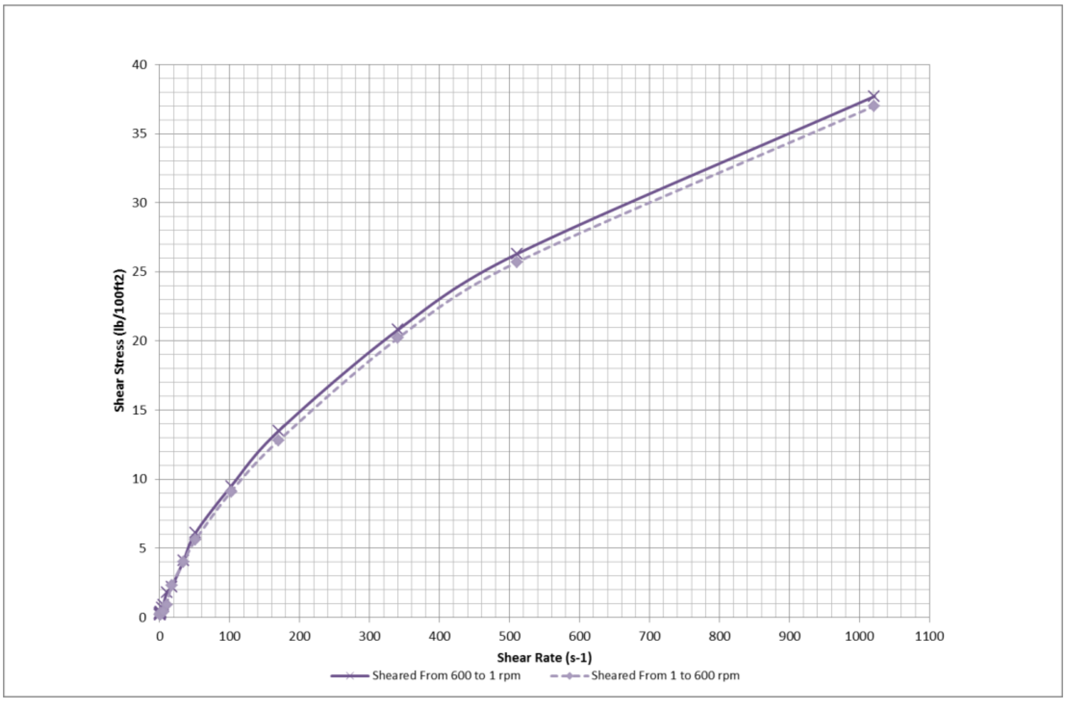

Figure 6.12 - Shear Stress - Shear Rate Graphic of 1.00 lb/bbl PAC Solution @ 60 ˚F

For analyzing the thixotropic behavior of PAC samples flow curves like Figure 6.12 are constructed by decreasing and then increasing shear rate values. It can be observed that PAC exhibits pseudoplasticity; shear stress is built back quickly even after higher applied shear rates. This quality helps mixing and pumping properties of the drilling or completion fluid after PAC has been added.

Figure 6.13 shows the effect of concentration on viscosity of the PAC R solution under constant temperature and shear rate. Increasing the amount of PAC R present in the solution increases the viscosity value as expected. It can be seen the effect of concentration is more visible when the applied shear rate is lower. This increase can be attributed to the intermolecular forces and entanglement of Polyanionic cellulose molecules. It is also seen that there isn’t any limiting concentration value present in the selected experiment range.

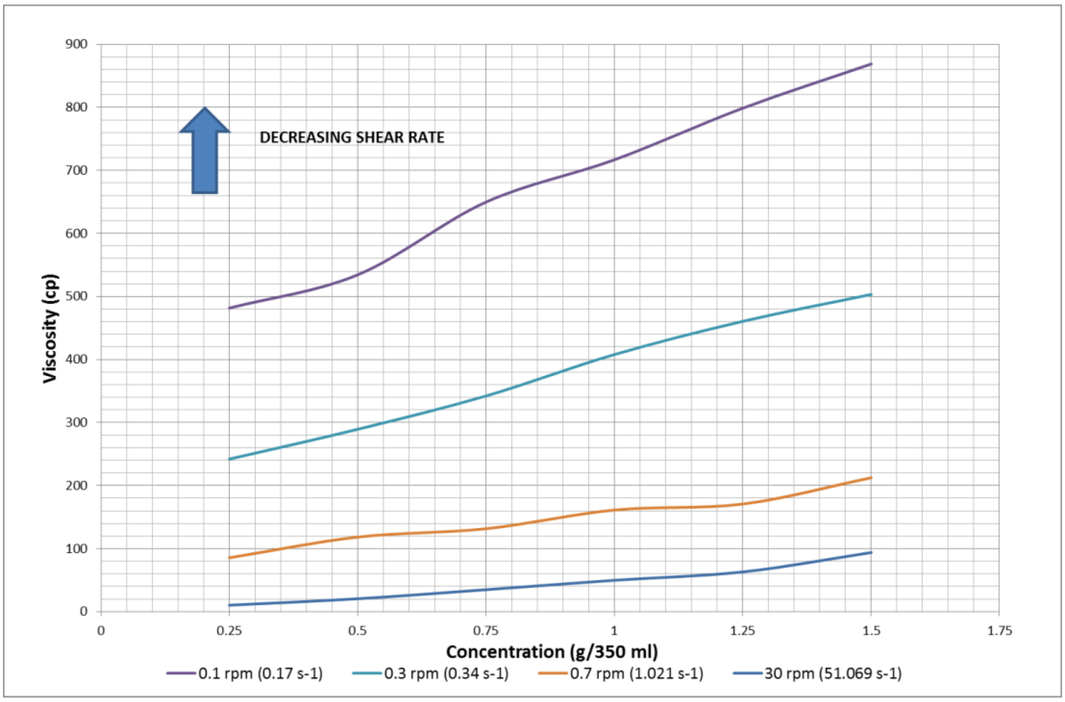

Figure 6.13 - Effect of Concentration on Apparent viscosity of PAC Solution @ 60 ˚F

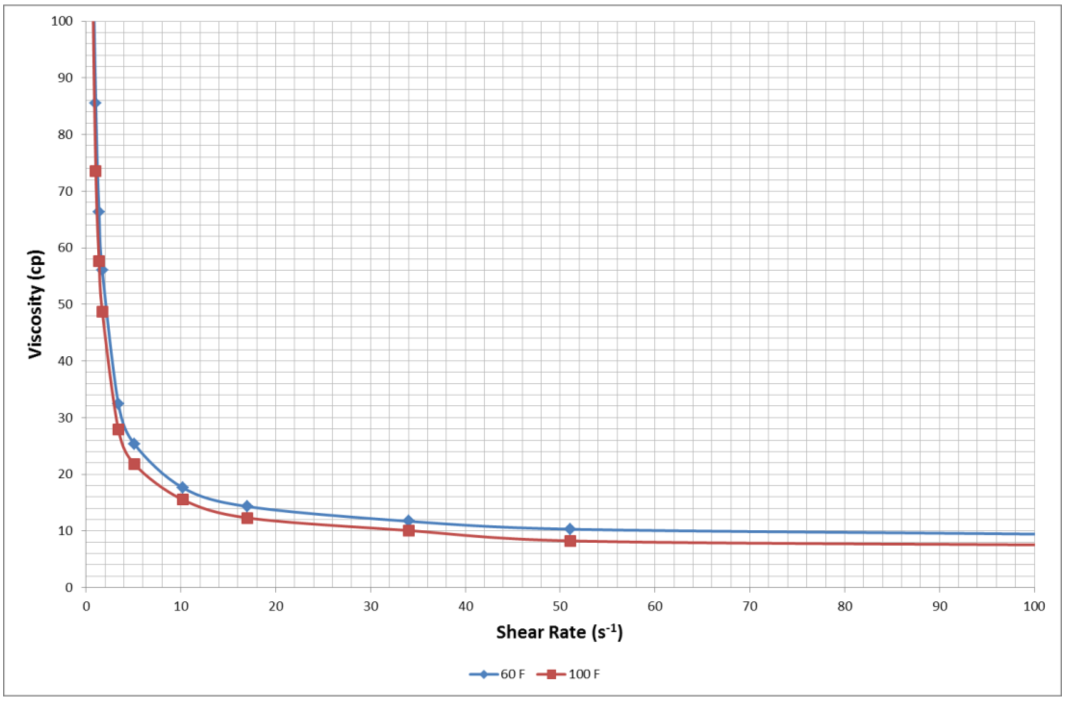

Figure 6.14 - Effect of Temperature on Apparent viscosity of 0.25 lb/bbl PAC Solution

Increasing temperature of the solution decreases apparent viscosity values just like xanthan gum solutions. The effect of temperature on PAC viscosity can be seen in Figure 6.14.

6.2.2 MATHEMATICAL MODELING OF POLYANIONIC CELLULOSE RHEOLOGY

The rheograms of PAC R obtained by experimental means are mathematically modeled akin to what is done in section 6.1.2 Mathematical Modeling of Xanthan Gum Rheology. Lower shear rate measurements are directly included in the calculations unlike the process in xanthan gum rheological modeling calculations. The purpose of adding lower shear rate measurements later was to emphasize the change of Herschel–Bulkley (or any other) mathematical model parameters upon inclusion of lower shear rate measurements.

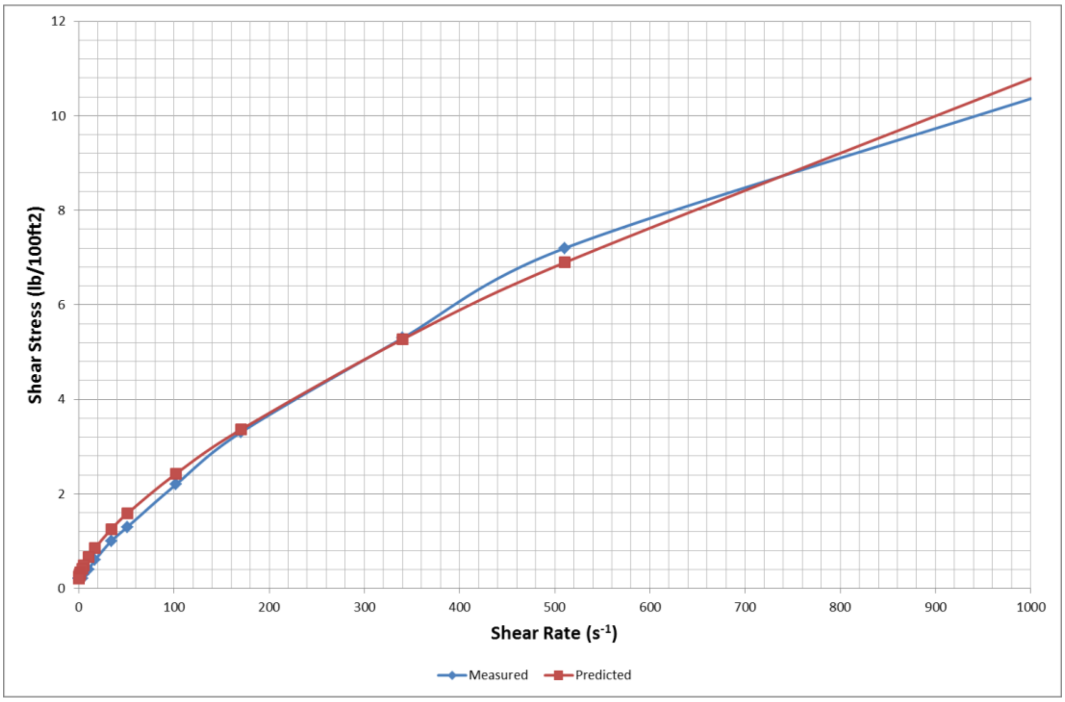

Figure 6.15 – Measured and Hershel–Bulkley Model Predicted Values for 0.25 lb/bbl PAC Solution @60 ˚F (with inclusion of low shear rate values)

Table 6.6 – Computed Herschel–Bulkley Rheological model parameters for PAC Solution at 60 °F (with inclusion of low shear rate parameters)

Concentration (lb/bbl)	τ_y (lb/100ft^2)	K (lb-s^n/100ft^2)	n (-)
0.25	0.20	0.09417	0.68383
0.50	0.21	0.17015	0.68334
0.75	0.23	0.2862	0.65911
1.00	0.26	0.4290	0.63871
1.25	0.29	0.6145	0.61863
1.50	0.32	1.0061	0.58543

The effect of concentration on computed Herschel–Bulkley model parameters were defined mathematically as follows:

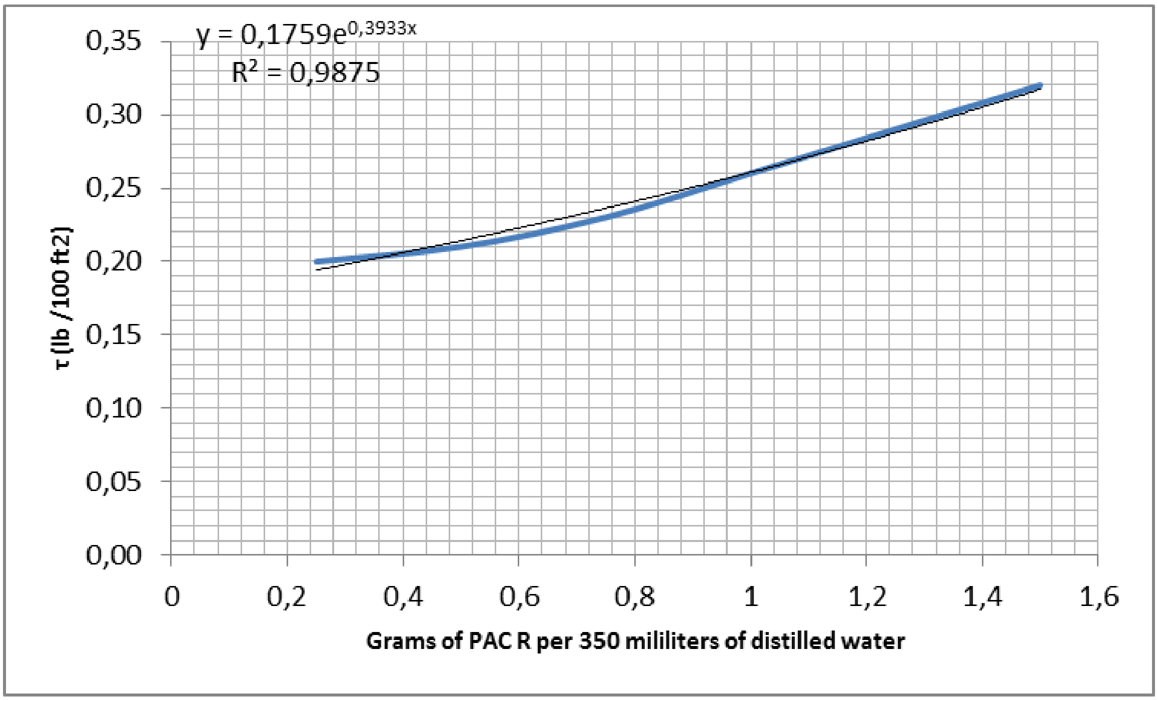

Figure 6.16 – Effect of Concentration of PAC on Yield Stress @ 60°F

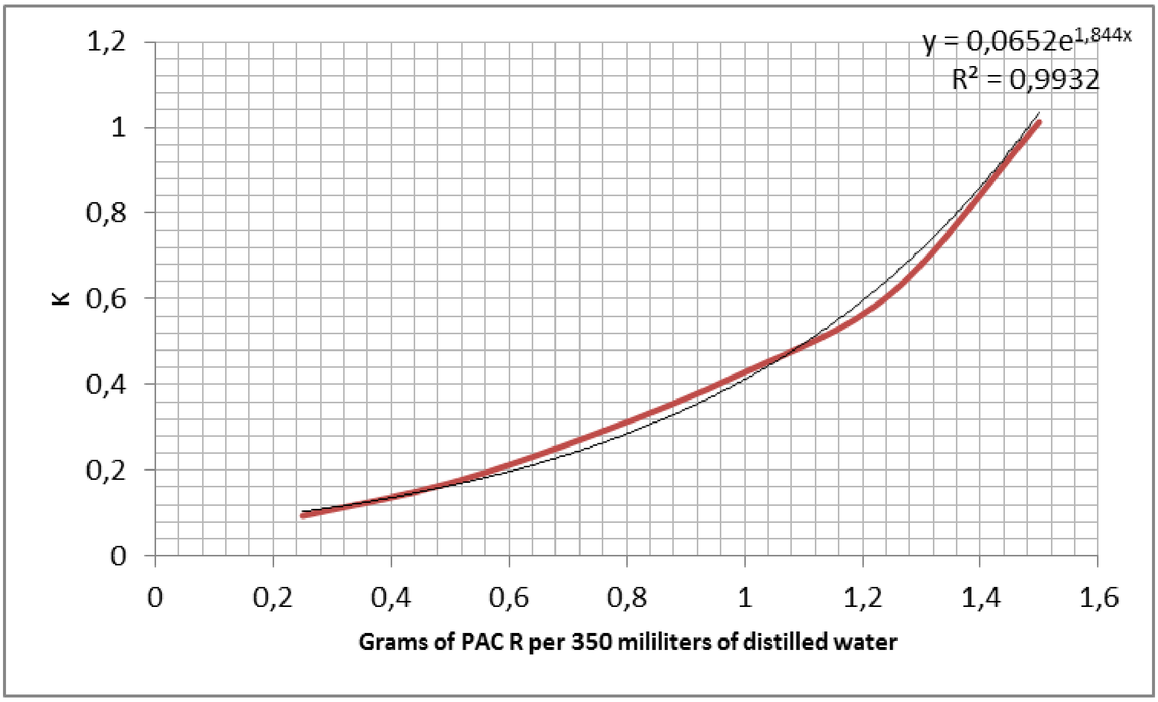

Figure 6.17–Effect of Concentration of PAC on K @ 60°F

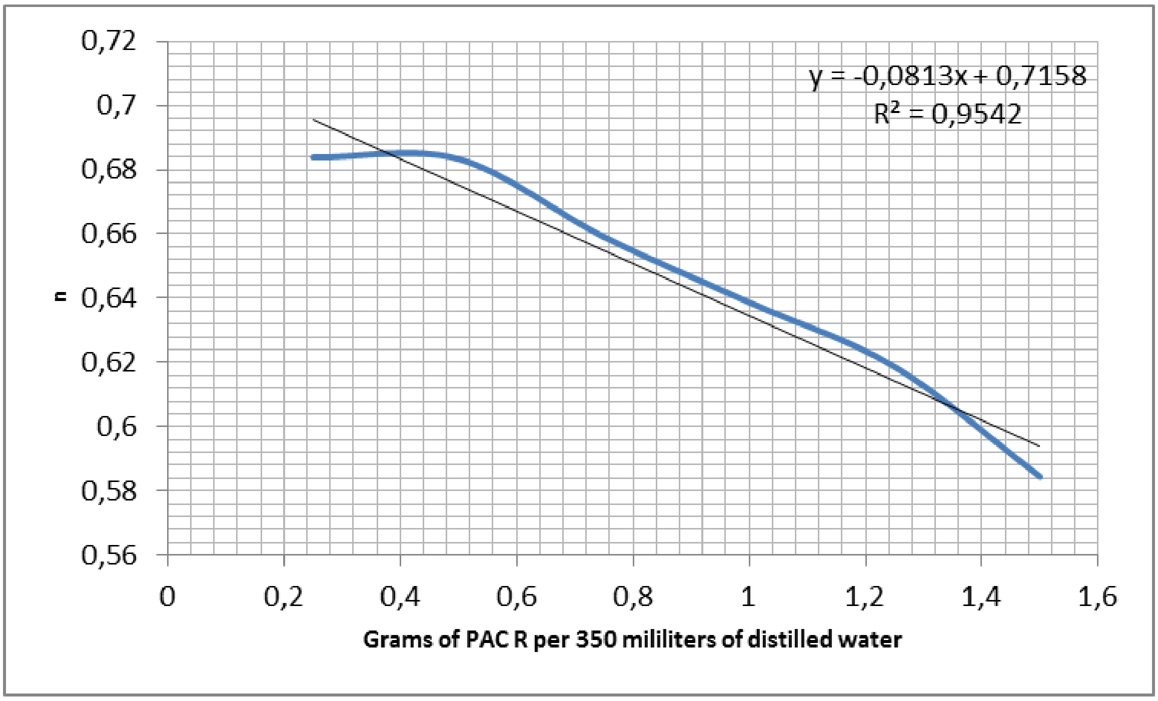

Figure 6.18 – Effect of Concentration of PAC on n @ 60°F

$$\tau_y = 0.1759e^{0.3933C} \text{ (a)}$$
$$K = 0.0652e^{1.844C} \text{ (b)} \qquad (6.5)$$
$$n = -0.0813\,C + 0.7158 \text{ (c)}$$

After all of the equations in Table 6.6 is put in Herschel–Bulkley rheological model, the combined equation becomes:

$$\boldsymbol{\tau} = 0.1759e^{0.3933C} + 0.0652e^{1.844C}\gamma^{(-0.0813C+0.7158)} \qquad (6.6)$$

Table 6.7 shows the predicted shear stress values for 0.25 grams of PAC R solution by different rheological models and compare their respective accuracies. It can be seen that Hershel–Bulkley model gives realistic estimates throughout the shear rate range.

Table 6.7 – Measured and Predicted Shear Stress Values for 0.25 lb/bbl PAC Solution @ 60 °F

Shear Rate (s^{-1})	Shear Stress (lb/100 ft^2)	Bingham Shear Stress (lb/100 ft^2)	Power Law Shear Stress (lb/100 ft^2)	Hershel- Bulkley Shear Stress (lb/100 ft^2)
1021.38	10.5	11.43518	10.84406	10.95692
510.69	7.2	5.81759	6.966458	6.896292
340.46	5.3	3.94506	5.377669	5.274788
170.23	3.3	2.07253	3.454732	3.359109
102.138	2.2	1.323518	2.493357	2.427705
51.069	1.3	0.761759	1.601787	1.58677
34.046	1	0.574506	1.236479	1.250964
17.023	0.6	0.387253	0.794341	0.854236
10.214	0.4	0.312354	0.573301	0.661353
5.107	0.4	0.256177	0.368301	0.487197
3.405	0.4	0.237455	0.284323	0.417667
1.702	0.3	0.218722	0.182621	0.335473
1.362	0.3	0.214982	0.158403	0.316324
1.021	0.3	0.211231	0.131785	0.295518
0.681	0.2	0.207491	0.101762	0.272413
0.34	0.2	0.20374	0.065313	0.245033
0.17	0.2	0.20187	0.041958	0.228033
0.153	0.2	0.201683	0.039229	0.226085
0.119	0.2	0.201309	0.033414	0.221966
0.085	0.2	0.200935	0.026955	0.217451
0.063	0.2	0.200693	0.022264	0.214219
0.051	0.2	0.200561	0.019454	0.212306
0.017	0.2	0.200187	0.009647	0.205806
Mean Square Error		0.340408	0.037136	0.029751

Table 6.8 – Measured and Predicted Shear Stress Values for 0.5 lb/bbl PAC Solution @ 100 °F

Shear Rate (s^{-1})	Shear Stress ($lb/100\ ft^2$)	Bingham Shear Stress ($lb/100\ ft^2$)	Power Law Shear Stress ($lb/100\ ft^2$)	Hershel- Bulkley Shear Stress ($lb/100\ ft^2$)
1021.38	16.9	19.02044	16.14837	16.62802
510.69	11.4	9.598206	10.39931	10.54912
340.46	9.1	6.457462	8.039043	8.095784
170.23	6.0	3.316719	5.177027	5.168398
102.138	3.6	2.060421	3.743076	3.728656
51.069	2.1	1.118198	2.410487	2.414339
34.046	1.6	0.804124	1.863393	1.883905
17.023	0.9	0.490049	1.199998	1.250976
10.214	0.7	0.364423	0.867629	0.93970
5.107	0.4	0.270199	0.558740	0.655528
3.405	0.3	0.238797	0.431953	0.540866
1.702	0.3	0.207377	0.278120	0.403964
1.362	0.3	0.201104	0.241426	0.371781
1.021	0.3	0.194812	0.201060	0.336648
0.681	0.2	0.188539	0.155475	0.297379
0.34	0.2	0.182248	0.100030	0.250381
0.17	0.2	0.179112	0.064418	0.220820
0.153	0.2	0.178798	0.060250	0.217404
0.119	0.2	0.178171	0.051364	0.210161
0.085	0.2	0.177543	0.041484	0.202178
0.063	0.2	0.177137	0.034300	0.196429
0.051	0.2	0.176916	0.029994	0.193010
0.017	0.2	0.176289	0.014932	0.181262
Mean Square Error		1.202438	0.18587	0.146165

Herschel-Bulkley model for polyanionic cellulose solutions at 100 °F as a function of concentration and shear rate become:

$$\boldsymbol{\tau} = (0.1514\,C^2 - 0.145C + 0.205) + (0.0648e^{1.8573C})\gamma^{(-0.0609C^2+0.0259C+0.6674)} \qquad (6.7)$$

Table 6.9 – Measured and Predicted Shear Stress Values for 0.75 lb/bbl PAC Solution @ 120 °F

Shear Rate (s^{-1})	Shear Stress (lb/100 ft^2)	Bingham Shear Stress (lb/100 ft^2)	Power Law Shear Stress (lb/100 ft^2)	Hershel- Bulkley Shear Stress (lb/100 ft^2)
1021.38	23.8	26.79369	23.41453	20.72114
510.69	15.7	13.49152	15.58104	13.79182
340.46	12.7	9.057458	12.27787	10.88036
170.23	8.6	4.623401	8.170224	7.272044
102.138	5.4	2.849778	6.051637	5.418207
51.069	3.2	1.519561	4.027021	3.653224
34.046	2.4	1.076155	3.173295	2.911638
17.023	1.3	0.632749	2.111648	1.992556
10.214	0.9	0.455392	1.564103	1.520376
5.107	0.6	0.322368	1.040822	1.070808
3.405	0.5	0.278035	0.820215	0.881955
1.702	0.3	0.233676	0.545713	0.647757
1.362	0.3	0.22482	0.478733	0.590785
1.021	0.3	0.215938	0.40416	0.527456
0.681	0.2	0.207082	0.31857	0.454929
0.34	0.2	0.198199	0.211807	0.364767
0.17	0.2	0.193771	0.140946	0.305186
0.153	0.2	0.193329	0.132484	0.298091
0.119	0.2	0.192443	0.114295	0.282856
0.085	0.2	0.191557	0.093791	0.265712
0.063	0.2	0.190984	0.078655	0.253083
0.051	0.2	0.190672	0.069471	0.245432
0.017	0.2	0.189786	0.036428	0.218011
Mean Square Error		2.482651	3.938684	0.923565

Herschel-Bulkley model for polyanionic cellulose solutions at 120 °F as a function of concentration and shear rate become:

$$\boldsymbol{\tau} = (0.1271\ e^{0.52355C}) + (0.0617e^{2.2561C})\gamma^{(-0.1398C+0.6988)} \qquad (6.8)$$

6.3 COMPARISON OF POLYANIONIC CELLULOSE AND XANTHAN GUM RHEOLOGY

When low end rheology of XCD and PAC are compared, it is clearly observed, as it can be also seen in Figure 6.19, that XCD provides much higher viscosities at lower shear rates, whereas PAC has additional benefits like providing water loss control, and a higher apparent viscosity profile at higher shear rates.

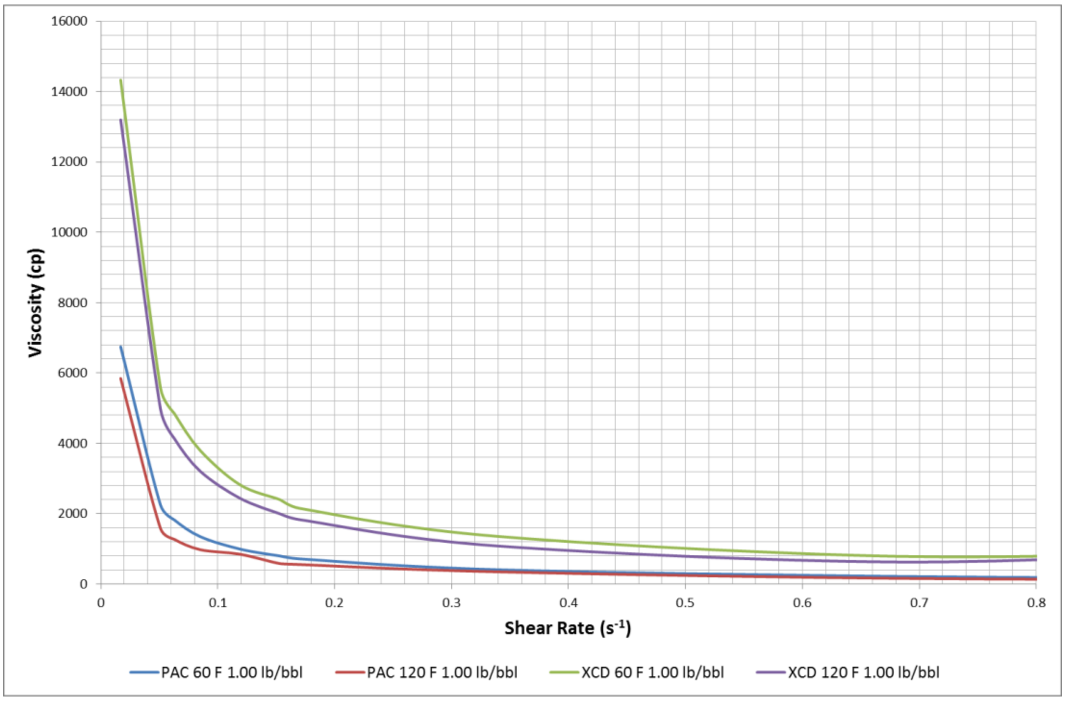

Figure 6.19 – Low Shear Rate Apparent Viscosity of XCD and PAC

It can also be observed that increasing solution temperature results in a similar magnitude of decrease in both XCD and PAC apparent viscosities.

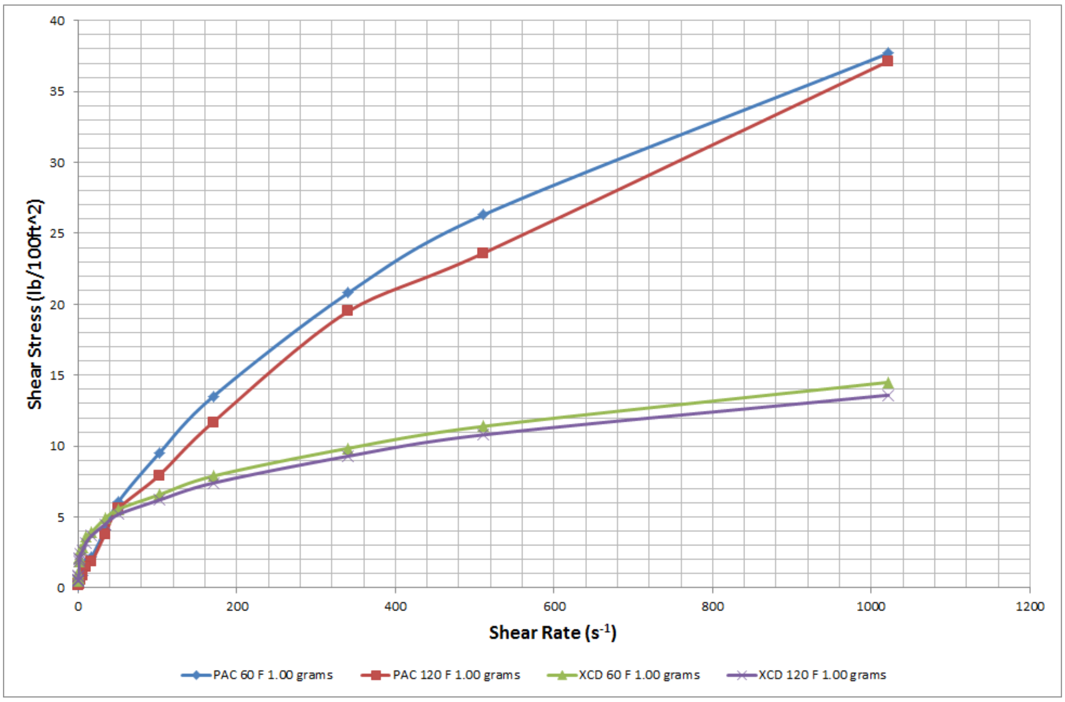

Figure 6.20 – Shear Stress Comparison of XCD and PAC

CHAPTER 7

CONCLUSION

This research was conducted in order to rheologically characterize some of the commonly used water soluble polymer used in drilling and completion operations. Measurements were made with the use of an Ofite Model 900 Low Shear Rate viscometer under atmospheric pressure.

Shear stress and shear rate relationship of the polymers were investigated by constructing rheograms. Effects of temperature and polymer concentration on viscosity were also analyzed by constructing appropriate diagrams. Based upon the work performed for this thesis the following conclusions were drawn:

1. Xanthan gum and PAC R solutions are highly pseudoplastic, shear-thinning fluids. This behavior is beneficial for suspending and hole cleaning capabilities of drilling and completion fluids, especially when pumping stops or decreases to lower rates.

2. Apparent viscosity of both polymer solutions consistently tends to increase with increasing polymer concentration because of intermolecular interaction as expected.

3. A significant reduction in apparent viscosity of xanthan gum and polyanionic cellulose solutions are measured with increasing

temperature and this behavior was observed to be reversible under the investigated temperature range.

4. Herschel–Bulkley rheological model more accurately describes the xanthan gum and PAC solutions’ rheology compared to two parameter models such as Bingham Plastic model and Power Law model.

5. Effect of concentration on xanthan gum and polyanionic cellulose solutions were mathematically modeled. Acceptably complex and accurate equations have been developed for both polymers, with today’s available computational power.

6. Xanthan gum shows quite higher apparent viscosity values at lower shear rates than PAC while PAC is providing superior apparent viscosity values at higher shear rates. The increased lower shear rate apparent viscosity of xanthan gum solutions is provided by the branched structure and a high tendency to form hydrogen bonds with water.

CHAPTER 8

RECOMMENDATIONS

These are some ideas which were not pursued because of time, money or equipment restrictions. They may be used as guidelines or recommendations for future work on the subject.

1- A vane rheometer can be used to conduct shear stress sweeps to measure dynamic yield stress values. Measured dynamic yield stress values can be compared and analyzed for any differences with the obtained yield stress values from Ofite Model 900 viscometer.

2- Measurements with standard six speed viscometers can be made so that they can be compared with the values obtained by using the low shear rate viscometer. It can be investigated that whether six speed viscometer measurements can be correlated to make estimation on low shear rate rheology.

3- With an appropriate test setup, effect of HP-HT on rheological behavior of polymeric solutions can be explored.

4- Rheology of these polymers can be investigated under different chemical environments with changing the solution pH and ionic nature.

5- Drilling and completion fluids are a mixture of variety of additives. This study can be extended to investigate rheological characteristics of different singular/mixture of additives.

REFERENCES

1. Schramm, G.: *A Practical Approach to Rheology and Rheometry*. Gebrueder HAAKE GmbH, Karlsruhe (1998), pp.11
2. Khodja, M., Khodja-Saber, M., Canselier, J. P., Cohaut, N., Bergaya, F.: Drilling Fluid Technology: Performances and Environmental Considerations. In : Products and Services; from R&D to Final Solutions. Sciyo, Rijeka (2010)
3. Kelco Oilfield Group: Rheology. Technical Bulletin, KOFG (2006)
4. Zamora, M., Power, D.: Drilling Fluid Yield Stress: Measurement Techniques for Improved Understanding of Critical Drilling Fluid Parameters. In : AADE National Technology Conference "Practical Solutions for Drilling Challanges", Texas (2003)
5. Shah, S., Shanker, N., Ogugbue, C.: Future Challenges of Drilling Fluids and Their Rheological Measurements. In : AADE Fluids Conference and Exhibiton, Houston (2010)
6. Slatter, P. T.: A New Friction Factor for Yield Stress Fluids. In : Hydrotransport 14, 14th International Conference on Slurry Handling and Pipeline Transport, Maastricht, 8-10 (1999)
7. Bharucha, V.: Rheological Study of Hydroproxypropyl Guar (HPG) Slurries. Master of Science Thesis, University of Oklahoma, Oklahoma (2004)
8. Becker, T. E., Morgan, R. G., Chin, W. C., Griffith, J. E.: Improved Rheology Model and Hydraulics Analysis for Tomorrow's Wellbore Fluid Applications. In : SPE Production and Operations Symposium, Oklahoma (2003)

9. Merlo, A., Maglione, R., Piatti, C.: An Innovative Model for Drilling Fluid Hydraulics. In : SPE Oil and Gas Conference, Kuala Lumpur (1995)
10. Saasen, A. L., Marken, C.: Prediction of Barite Sag Potential of Drilling Fluids from Rheological Measurements. In : IADC Drilling Conference, Amsterdam (1995)
11. Bern, P., Zamora, M., Slater, K., Hearn, P.: The Influence of Drilling Variables on Barite Sag. In : SPE Acte, Denver (1996)
12. Dye, W., Hemphill, T., Gusler, W., Mullen, G.: Correlation of Ultralow-Shear-Rate Viscosity and Dynamic Barite Sag., 27 - 34 (2001)
13. Powell, J. V., Parks, C. F., Seheult, J. M.: Xanthan and Welan: The Effects of Critical Polymer Concentration on Rheology and Fluid Performance. In : International Arctic Technology Conference, Alaska (1991)
14. Becker, T. E., Azar, J. J., Okrajni, S. S.: Correlations of Mud Rheologic Properties With Cutting Transport Performance in Directional Drilling. In : 64th Annual Technical Conference and Exhibition of the SPE, Texas (1989)
15. Gavinet, A. A., Sobey, I. J.: A Model for Transport of Cuttings in Highly Deviated Wells. In : 61st Annual Technical Conference and Exhibition of the SPE, New Orleans (1996)
16. Saasen, A., Eriksen, N. H., Han, L., Labes, P., Marken, C. D.: Good Hole Cleaning - Is Annular Friction Loss the Key Parameter. Oil Gas European Magazine 1(24), 22 - 24 (1998)
17. Karkim Sondaj Akışkanları, Enerji ve Mühendislik Hizmetleri. Available at: http://www.karkim.com/
18. Viswanath, D., Ghosh, T., Prasad, D., Dutt, N., Rani, K.: *Viscosity of Liquids: Theory, Estimation, Expertiments and Data*. Springer, Dordrecht (2007), pp.61

19. Morton, K. E., Balestrini, A., Maas, T., Seheult, M.: Advances in API/ISO Standard Grade Purified Poly-Anionic Cellulose (PAC) and Drilling Grade Xanthan Gum (XG) Test Procedure and Specifications Definition. In : SPE/IADC Drilling Conference and Exhibition, Amsterdam (2009)
20. Lipton, D., Burnett, D. B.: Comparisons of Polymers Used in Workover and Completion Fluids. In : 46th Annual Regional Meeting of the Society of Petroleum Engineers of AIME, California (1976)
21. Oviatt, H. W., Brant, D. A.: Thermal treatment of semi-dilute xanthan solutions yields weak gels with properties resembling hyaluronic acid. Int. J. of Biol. Macromol.(15), 3 - 10 (1993)
22. Garcia-Ochoa, F., Santos, V. E., Casas, J. A., Gomez, E.: Xanthan Gum: Production, Recovery and Properties. Biotechnology Advances(18), 549 - 579 (2000)
23. Hemphill, T.: New Visccometer Allows for Improved Understanding of Drilling Fluid Behavior at Low Shear Rates. In : AADE Annula Technical Forum - Improvements In Drilling Fluids Technology, Houston (1999)
24. Barnes, H., Hutton, J., Walters, F. R.: *An Introduction to Rheology*. Elsevier, Amsterdam (1993)
25. Thivolle, S.: A New Practical Rheology Model for HPHT Fluid., paper presented for M. Eng. degree Texas A&M University. College Station, Texas (2004)
26. Macosko, C. W.: *Rheology: Principles, Measurements and Applications*. John Wiley & Sons (1994)
27. Morton , K., Balestrini, A., Maas, T., Seheult, M.: Advances in API/ISO Standard Grade Purified Poly-Anionic Cellulose (PAC) and Drilling Grade Xanthan Gum (XG) Test Procedure and Specifications Definition. In : SPE/IADC Drilling Conference and Exhibiton , Amsterdam (2009)

APPENDIX A

ABBREVIATION GUIDE FOR ORCADA^{TM} TEST BUILDER

- "Heat Time" is the amount of time which will be taken to heat the drilling fluid sample to the required temperature by the viscometer heating cup. If this field is blank, the sample will be heated as fast as possible.

- "Heat RPM" is amount of rotations performed in a minute by the rotor during heating periods.

- "Temp" is the required temperature value for the drilling fluid sample to reach. Any letter entered in this field will result in operation at ambient temperature.

- "Cond. Time" is the period of time for conditioning the fluid sample before taking readings.

- "Cond. RPM" is the rotational speed during the conditioning period.

- "#/Swps" is the number of set rotational speed intervals. Between each sweep the rotor returns to conditioning rpm.

- "Delta Time" is the value of the time interval between each sweep.

- “Gel Time” can be added by right clicking the insert gel column button. The rotor comes to a stop until the end of this interval, then starts to turn at 3 rpms until the gel breaks and a gel strength value is recorded.

- “RPM #” sets the amount of rotations per minute for each respective step of the sweep.

- “Hold for Temp” checkbox instructs the viscometer to the set temperature before reaching the next step of the test. If this checkbox is left as is the test will continue while the sample is still heating.

- “Temp Threshold” field specifies the amount of acceptable deviation from the set temperature.

- “Temp Unit” field is used for temperature unit, either C^{o} or F°.

- “Rate Unit” field is used to fix the rate units to either rpm or 1/s.

- “Hystoresis” field can be checked to perform sweeps on both directions; forward and backward.

- “Stir Prior to Gel” checkbox can be used to stir the sample before calculating gel strength.

- “Gel Stir Rate” is the set rate at which the sample will be stirred to prior gel strength calculation.

- “Gel Stir Time” is the interval the sample will be stirred.

APPENDIX B

SHEAR RHEOLOGY

NEWTONIAN RHEOLOGY

Rheology deals with the study of flow and deformation of materials. Simple shear flow can be defined as the continual movement of liquid particles over or past each other. Consider a thin layer of fluid contained between two parallel planes with some distance between as shown in Figure B.1. If the fluid is subjected to shear by application of a force F as shown, the internal resistance to flow of the fluid between the plates will create force balance. For an incompressible Newtonian fluid in laminar flow, the resulting shear stress is equal to the product of the shear rate and viscosity of the medium. For this case shear rate can be considered as the velocity gradient in the direction perpendicular to the direction of the shear force.

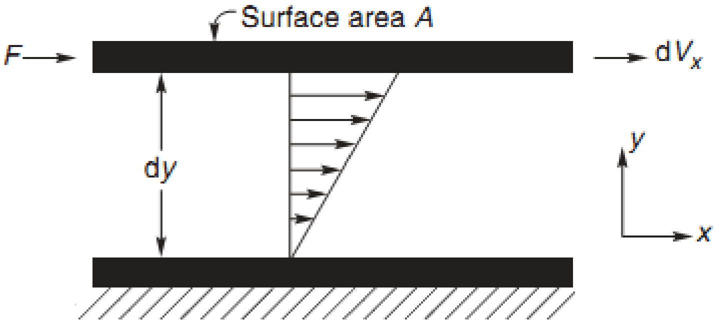

Figure B. 1 – Schematic representation of unidirectional shearing flow

$$\frac{F}{A} = \tau_{yx} = \mu\left(-\frac{dV_x}{dy}\right) = \mu\gamma_{yx} \qquad \text{(B.1)}$$

The first subscript on both the shear rate and shear stress indicates the direction normal to that of shearing surface, whereas the other subscript refers to the direction of the force and the resulting flow.

The constant of proportionality, μ (the ratio of shear stress to shear rate), is called the Newtonian viscosity and is independent of shear stress and shear rate, only depending on the material, temperature and pressure. So the flow curve or rheogram of a Newtonian fluid will be a straight line of slope, μ, passing through the origin. At constant temperature and pressure viscosity defines the flow behavior of the Newtonian fluid. Gases, simple organic liquids, solutions of low molecular weight inorganic salts, molten metals and salts are all Newtonian fluids.

NON-NEWTONIAN FLUID RHEOLOGY

The flow curve of a non-Newtonian fluid is not linear or it does not pass through the origin. The apparent viscosity of such fluids at a constant pressure and temperature can depend on conditions such as flow geometry, shear rate, flow history of the fluid, etc. This kind of fluids can be divided into three classes:

1- Time independent fluids: Fluids for which the rate of shear at any point is only determined by the value of the shear stress at that point at that instant.

2- Time dependent fluids: Fluids for which the rate of shear also depends upon the duration of shear and kinematic history of the fluid.

3- Viscoelastic fluids: Substances exhibiting both characteristics of ideal fluids and elastic solids and showing partial elastic recovery.

TIME INDEPENDENT FLUID BEHAVIOR

The flow behavior of time independent fluids can be expressed with a constitutive equation of the following form:

$$\tau_{yx} = f(\gamma_{yx}) \qquad \text{(B.2)}$$

This equation implies that value of shear rate at any point within the sheared fluid is determined only by the value of the shear stress or vice versa.

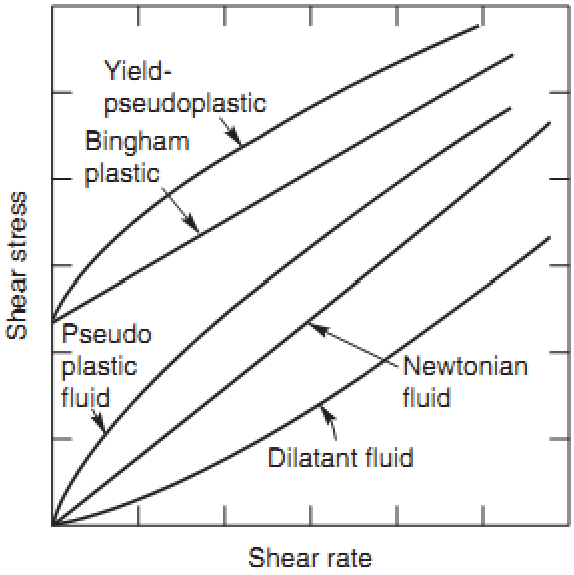

Figure B. 2 – Types of Time-Independent Fluid Flow Behavior

It can be seen in Figure B.2 that time independent fluids show different kinds of flow behavior.

SHEAR THINNING (PSEUDOPLASTIC) FLUIDS

This is the most common type of time independent non-Newtonian fluid flow behavior encountered. Apparent viscosity values gradually decrease with increasing shear rate. At sufficiently low shear rate values the apparent viscosity of the polymeric systems approach a Newtonian plateau where the viscosity is independent of the shear rate, the so-called zero shear rate viscosity (μ_0). Polymer solutions also exhibit a similar behavior at very high shear rates (infinite shear rate viscosity, μ_∞).

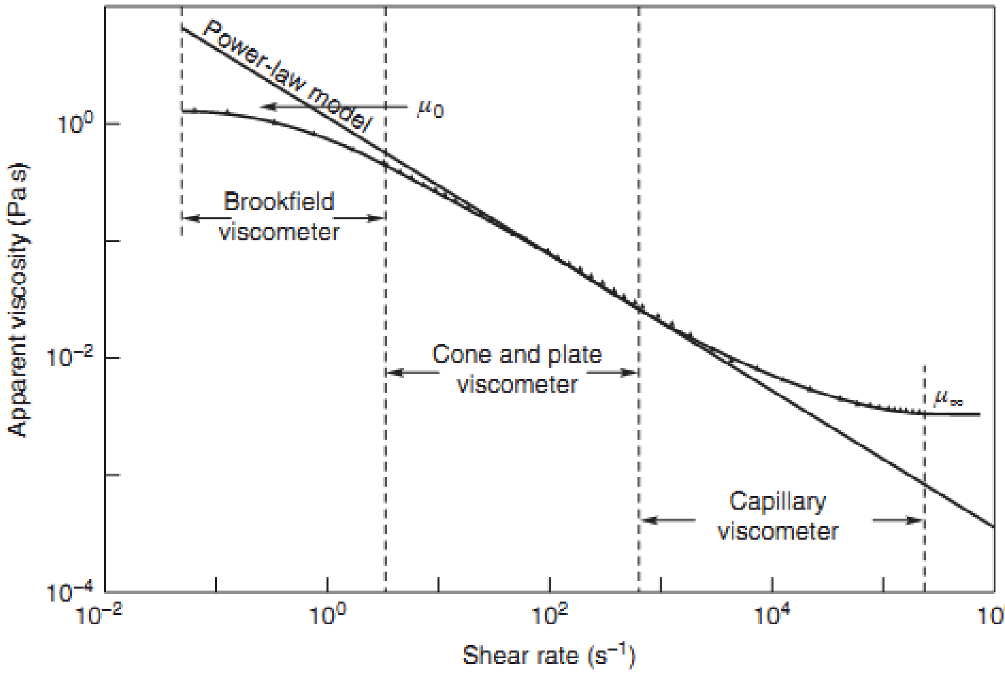

Figure B. 3 – Graphical Representation of Zero and Infinite Shear Viscosities for a Shear Thinning Polymer Solution

SHEAR THICKENING (DILATANT) FLUIDS

Dilatant fluids exhibit apparent viscosity increase with increasing shear rate. This behavior is generally observed in concentrated suspensions. At rest the liquid present in the sample is sufficient to fill the voids completely. At low shearing levels, the liquid lubricates the motion of each particle past another thereby minimizing solid-solid friction. Consequently, the resulting stresses are small. At high shear rates, however, the mixture expands (dilates) slightly so that the available liquid is no longer sufficient to fill the increased void space and to prevent direct solid-solid contacts (and friction). This leads to the development of much larger shear stresses than that seen in a pre-dilated sample at low shear rates. This mechanism causes the apparent viscosity to rise rapidly with the increasing rate of shear.

VISCOPLASTIC FLUID BEHAVIOR

These kinds of fluids exhibit a yield stress which has to be exceeded to initiate fluid flow or deformation. If a stress smaller than the yield stress is applied to the fluid, it will act like a rigid body and deform elastically. If the applied shear stress exceeds the yield stress the fluid will deform and the flow curve can be linear or non-linear.

A fluid with a linear flow curve for applied stresses bigger than the yield stress is called a Bingham Plastic fluid and has a constant plastic viscosity (the slope of the shear stress versus shear rate plot) and a yield stress. There are also fluids with a non-linear flow curves for applied stresses bigger than the yield stress which are called yield-pseudoplastic material.

Representative flow behavior of a Bingham Plastic fluid and a yield-pseudoplastic material can be seen in Figure B.4. It can be seen that a viscoplastic material also displays a decrease in apparent viscosity with increasing shear stress.

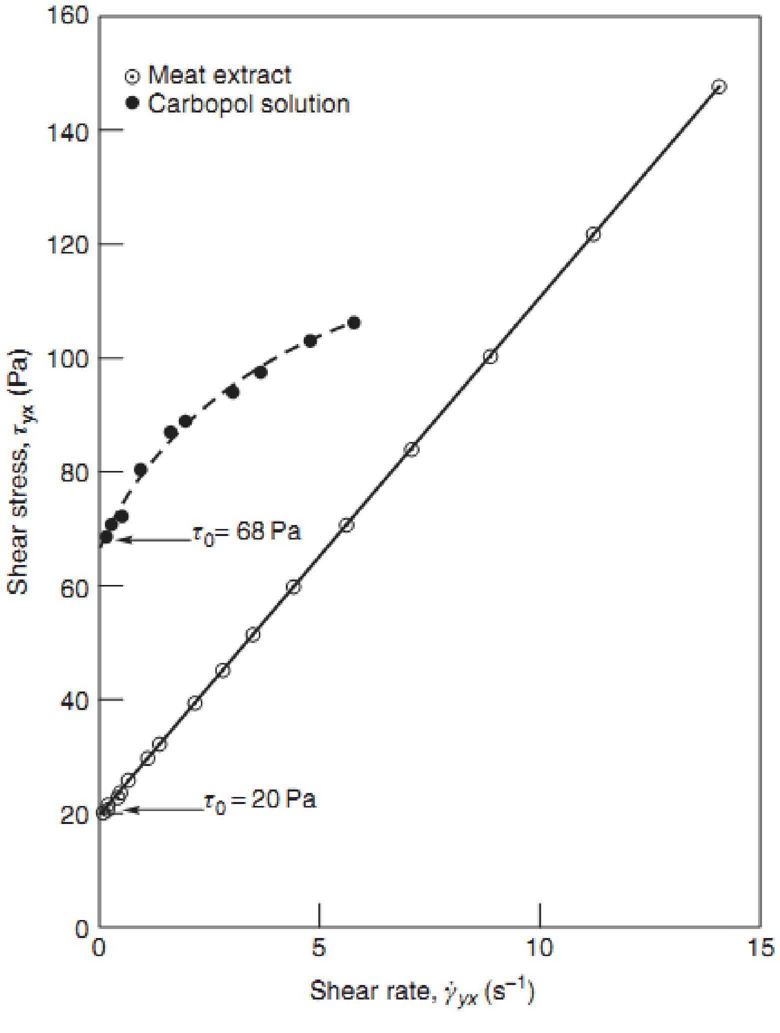

Figure B. 4 – Representative Shear Stress and Yield Stress Data; Meat Extract (Bingham Plastic) and an Aqueous Carbopol Polymer Solution (Yield-Pseudoplastic)

TIME DEPENDENT FLUID BEHAVIOR

An important thing to note in investigation of drilling fluids is the time dependence of the sample. Due to physical and/or chemical associations between the particles of the fluid time dependent behavior can be seen in response to an applied shear stress or strain. Viscosity of the sample fluid will change with time while being sheared at a constant rate. There are two possible behaviors for time dependent fluid behavior as can be seen in Figure B.5.

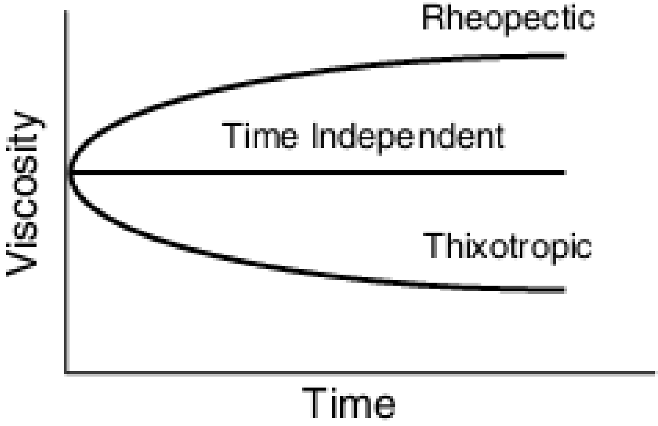

Figure B. 5 – Time Dependent Fluid Behavior

Time dependent rheological behavior is generally referred to as thixotropy and the degree of thixotropy of a fluid can simply be measured by performing a shear test where the shear rate is first increased to a maximum degree (up-sweep curve) and then decreased down (down-sweep curve). When then up-sweep curve of a shear stress versus shear rate plot is above the down-sweep curve, the fluid can be referred to as positively thixotropic. For the opposite condition, the fluid can either be called as negatively thixotropic or rheopectic.

RHEOLOGICAL MODELS

A myriad of mathematical models have been proposed to accurately describe shear stress and shear rate relation of non-Newtonian fluids. Rheological measurement and evaluation of drilling fluids are generally made with concentric cylinder viscometers and data measured with these viscometers are then used to find empirical model parameters. The most commonly used rheological models for describing the rheological behavior of drilling fluids are Bingham Plastic and Power Law models.

POWER LAW MODEL

In power law model, the viscosity term present in Newtonian model is replaced with a constant, K, named as the consistency index, which serves as an index for the viscosity of the system. Also the shear rate term is raised to the nth power hence the name power law. The parameter n, flow behavior index defines the tendency of the fluid to shear thin. Deviation of flow behavior index from one shows increasing non-Newtonian rheology. Although this is one of the most widely used rheological models, no known fluids exhibit power law behavior throughout all shear rates hence the validity of the model is limited over a shear rate range.

$$\tau = K\,\gamma^{n} \qquad \text{(B.3)}$$

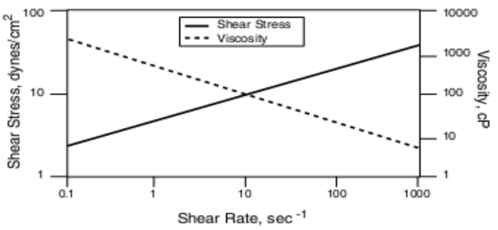

Figure B. 6 – Idealized Power Law Fluid

BINGHAM PLASTIC MODEL

Another widely used two parameter rheological model is the Bingham Plastic model. Bingham Plastic fluids are characterized by a yield stress and a shear rate independent plastic viscosity. Applied shear stress should exceed yield stress value before the fluid starts to flow and if the fluid exhibits Newtonian behavior after the flow is initiated, the fluid can be called a Bingham Plastic fluid. Bingham Plastic model has been used to describe a few clay based muds and cement slurries.

$$\tau = \tau_o + \mu_p \gamma \tag{B.4}$$

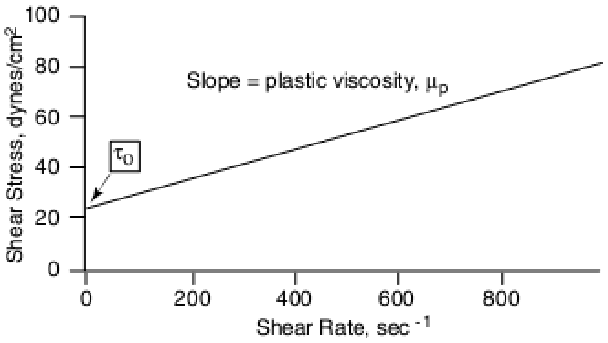

Figure B. 7 – Idealized Bingham Plastic Fluid

HERSCHEL–BULKLEY MODEL

Fluids which both have a yield point and shear rate dependent viscosity cannot be adequately described by Bingham Plastic model. Herschel–Bulkley model overcomes this deficiency by changing the plastic viscosity term in Bingham Plastic model with a power law expression.

$$\tau = \tau_o + K\, \gamma^n \tag{B.5}$$

Herschel–Bulkley and all other models which cannot be linearized easily by curve fitting techniques were not used in field because of the complex calculations. However with the increase of availability and ease of use of personal computers, these models are getting increasing attention and use.

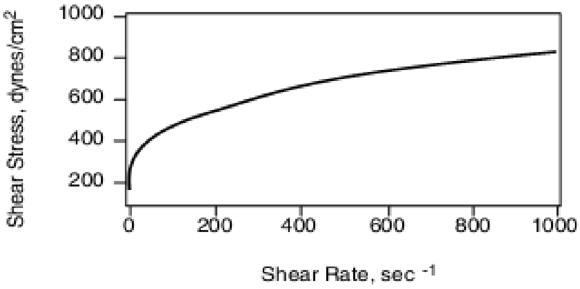

Figure B. 8 – Idealized Herschel – Bulkley Fluid

APPENDIX C

EXPERIMENT DATA FOR XCD

Table C. 1 – Shear Stress Values of XCD @ 60 °F

	Shear Stress (lb /100 ft^2)					
Shear Rate (s^{-1})	***0.25 lb/bbl***	***0.50 lb/bbl***	***0.75 lb/bbl***	***1.00 lb/bbl***	***1.25 lb/bbl***	***1.50 lb/bbl***
1021.38	5.3	9.0	12.0	16.5	20.0	25.8
510.69	4.0	6.6	9.4	12.7	15.7	20.3
340.46	3.3	5.4	7.7	10.9	13.9	17.5
170.23	2.3	4.3	6.2	8.7	11.3	14.2
102.138	2.0	3.5	5.2	7.3	9.9	12.8
51.069	1.8	2.5	4.3	6.3	8.4	10.7
34.046	1.3	2.1	3.9	5.7	7.4	10
17.023	0.8	1.6	2.8	4.6	6.4	8.6
10.214	0.7	1.4	2.4	4.3	5.9	7.6
5.107	0.5	1.2	2.2	3.5	4.9	6.6
3.405	0.4	1.1	1.9	3.1	4.6	6.2
1.702	0.4	0.9	1.6	2.3	4.1	5.3
1.362	0.3	0.9	1.5	2.2	3.9	5.1
1.021	0.3	0.9	1.3	1.9	3.5	4.9
0.681	0.3	0.8	0.9	1.6	2.8	4.4
0.34	0.3	0.7	0.7	1.3	2.2	3.4
0.17	0.3	0.6	0.6	1.0	1.6	2.6
0.153	0.3	0.6	0.6	1.0	1.5	2.6
0.119	0.3	0.5	0.6	0.9	1.4	2.3
0.085	0.3	0.5	0.6	0.8	1.2	2.0
0.063	0.3	0.5	0.5	0.8	1.1	1.9
0.051	0.3	0.4	0.5	0.7	1	1.7
0.017	0.3	0.4	0.5	0.6	0.8	1.5

Table C. 2 – Apparent Viscosity Values of XCD @ 60 °F

	Apparent Viscosity (cp)					
Shear Rate (s^{-1})	***0.25 lb/bbl***	***0.50 lb/bbl***	***0.75 lb/bbl***	***1.00 lb/bbl***	***1.25 lb/bbl***	***1.50 lb/bbl***
1021.38	2.5	4.2	5.7	7.8	9.4	12.1
510.69	3.8	6.2	8.8	12.0	14.8	19.0
340.46	4.7	7.6	10.8	15.3	19.6	24.7
170.23	5.8	12.1	17.5	24.6	31.8	40.1
102.138	8.3	18.0	24.5	34.4	46.6	60.2
51.069	12.7	21.9	40.4	58.8	79.0	101.0
34.046	14.6	30.2	54.6	80.3	103.7	141.6
17.023	21.8	46.4	78.9	130.9	181.1	242.6
10.214	31.7	72.6	113.8	201.7	277.2	358.7
5.107	49.0	122.3	177.5	328.7	459.2	617.8
3.405	61.5	151.9	247.3	430.6	653.7	877.3
1.702	101.4	265.6	445.8	650.1	1162.8	1504.9
1.362	123.1	319.6	470.3	759.7	1378.2	1813.2
1.021	155.8	404.7	524.6	903.9	1623.3	2281.2
0.681	220.2	562.8	627.4	1150.8	1966.4	3071.1
0.34	414.0	975.5	1040.9	1787.3	3097.4	4759.3
0.17	806.5	1574.0	1766.0	2879.5	4483.4	7478.0
0.153	880.1	1824.6	1942.7	3117.2	4704.0	8059.3
0.119	1112.8	1972.8	2395.0	3715.7	5446.8	9328.2
0.085	1557.6	2587.1	3133.3	4761.5	6902.7	11568.0
0.063	2101.6	3489.5	4014.9	5970.8	8511.7	14095.1
0.051	2596.1	4311.8	4793.7	7033.6	9871.9	15808.2
0.017	7788.2	9206.5	12285.0	16525.5	21398.5	27513.9

Table C. 3 – Shear Stress Values of XCD @ 100 °F

Shear Rate (s^{-1})	**Shear Stress (lb /100 ft^2)**					
	0.25 lb/bbl	***0.50 lb/bbl***	***0.75 lb/bbl***	***1.00 lb/bbl***	***1.25 lb/bbl***	***1.50 lb/bbl***
1021.38	4.1	7.7	10.7	14.5	18.5	21.3
510.69	3.1	5.5	8.7	11.4	14.6	17.2
340.46	2.6	4.7	7.1	9.9	13.0	15.3
170.23	2.2	3.4	5.1	7.9	10.5	13.1
102.138	1.9	2.8	4.3	6.6	9.5	11.7
51.069	1.7	1.9	3.5	5.6	7.6	10.1
34.046	1.2	1.7	3.2	4.9	6.8	9.5
17.023	0.4	1.4	2.5	4.0	5.7	7.9
10.214	0.4	1.2	2.1	3.6	5.0	7.0
5.107	0.4	0.9	1.9	2.9	4.3	5.9
3.405	0.3	0.7	1.7	2.7	4.0	5.3
1.702	0.3	0.7	1.4	2.2	3.5	4.5
1.362	0.3	0.7	1.3	2.1	3.3	4.2
1.021	0.3	0.4	1.1	1.9	3.0	3.9
0.681	0.3	0.4	0.7	1.1	2.6	3.5
0.34	0.3	0.4	0.5	0.9	2.1	2.9
0.17	0.3	0.3	0.4	0.7	1.1	2.3
0.153	0.3	0.3	0.4	0.8	1.1	2.1
0.119	0.3	0.3	0.4	0.7	1.1	2.0
0.085	0.3	0.3	0.4	0.7	0.9	1.8
0.063	0.3	0.3	0.4	0.6	0.9	1.7
0.051	0.3	0.3	0.4	0.6	0.8	1.5
0.017	0.3	0.3	0.4	0.5	0.7	1.2

Table C. 4 - Apparent Viscosity Values of XCD @ 100 °F

	Apparent Viscosity (cp)					
Shear Rate (s^{-1})	***0.25 lb/bbl***	***0.50 lb/bbl***	***0.75 lb/bbl***	***1.00 lb/bbl***	***1.25 lb/bbl***	***1.50 lb/bbl***
1021.38	2.0	3.6	5.3	6.9	8.7	10.6
510.69	2.8	5.2	8.1	10.8	13.7	17.2
340.46	3.7	6.3	10.2	14.0	18.3	22.5
170.23	5.5	9.6	13.8	22.1	29.5	37.8
102.138	8.2	13	20.7	31.1	44.7	56.8
51.069	12.2	17.4	34.1	51.9	71.3	93.0
34.046	14.3	24.3	41.5	68.4	97.4	130.6
17.023	20.0	45.8	67.8	113.6	160.8	223.1
10.214	27.0	71.3	103.3	168.5	239.2	330.4
5.107	34.9	118.1	142.5	267.8	405.1	553.7
3.405	46.8	144.5	236.3	367.0	570.0	774.9
1.702	88.5	223.3	329.2	619.5	976.3	1257.5
1.362	107.6	242.6	360.7	732.4	1155.8	1504.8
1.021	139.2	265.8	392.1	905.3	1432.9	1879.5
0.681	204.4	319.1	471.6	787.7	1851.5	2435.5
0.34	397.5	592.5	677.7	1354.0	2903.6	3781.7
0.17	787.2	984.3	1078.3	2153.2	3260.7	6399.4
0.153	873.2	1123.5	1218.5	2402.0	3452.3	6914.7
0.119	1028.6	1295	1499.2	2822.8	4091.9	8168.5
0.085	1372.4	1517.6	1843.7	3799.1	5405.0	10083.6
0.063	2078.5	2193.7	2763.4	4843.0	6795.3	11826.9
0.051	2345.8	2596.1	3209.7	5580.5	7896.1	13519.2
0.017	7342.5	8405.9	9201.7	14329.9	17915.7	24432.1

Table C. 5 - Shear Stress Values of XCD @ 120 °F

	Shear Stress (lb /100 ft^2)					
Shear Rate (s^{-1})	***0.25 lb/bbl***	***0.50 lb/bbl***	***0.75 lb/bbl***	***1.00 lb/bbl***	***1.25 lb/bbl***	***1.50 lb/bbl***
1021.38	3.5	7.1	10.3	13.6	17.6	19.1
510.69	2.6	5	7.7	10.8	14.0	14.7
340.46	2.3	4.1	6.8	9.3	12.6	12.7
170.23	2.1	2.7	4.6	7.4	10.1	11.8
102.138	1.8	1.8	4	6.2	9.3	10.1
51.069	1.4	1.5	3.2	5.2	7.2	9.5
34.046	1.1	1.3	2.8	4.5	6.6	8.8
17.023	0.3	1.1	2.3	3.7	5.4	7.5
10.214	0.3	0.8	2	3.2	4.6	6.7
5.107	0.3	0.6	1.8	2.6	4.0	5.6
3.405	0.3	0.4	1.6	2.4	3.7	5.0
1.702	0.3	0.4	1.2	2.1	3.2	4.0
1.362	0.3	0.3	1.1	2.0	3.0	3.8
1.021	0.3	0.3	0.9	1.9	2.8	3.6
0.681	0.3	0.3	0.8	0.9	2.5	3.0
0.34	0.3	0.3	0.7	0.8	2.0	2.4
0.17	0.3	0.3	0.5	0.6	0.9	2.1
0.153	0.3	0.3	0.5	0.6	0.9	2.0
0.119	0.3	0.3	0.4	0.6	0.9	1.9
0.085	0.2	0.3	0.4	0.6	0.8	1.6
0.063	0.2	0.3	0.3	0.5	0.8	1.4
0.051	0.2	0.2	0.3	0.5	0.7	1.3
0.017	0.2	0.2	0.3	0.5	0.6	1.0

Table C. 6 - Apparent Viscosity Values of XCD @ 120 °F

	Apparent Viscosity (cp)					
Shear Rate (s^{-1})	***0.25 lb/bbl***	***0.50 lb/bbl***	***0.75 lb/bbl***	***1.00 lb/bbl***	***1.25 lb/bbl***	***1.50 lb/bbl***
1021.38	1.7	3.2	4.9	6.4	8.3	10.0
510.69	2.4	5.2	7.2	10.2	13.1	16.2
340.46	3.3	6.3	9.6	13.2	17.7	21.5
170.23	5.3	8.4	13.0	20.8	28.5	36.9
102.138	8.1	11.2	18.9	29.2	43.8	55.3
51.069	12.0	15.6	30.3	48.7	67.9	89.1
34.046	14.2	22.7	39.8	63.8	93.7	123.4
17.023	19.1	44.6	63.7	103.6	151.6	211.1
10.214	24.5	70.6	95.4	149.3	216.6	313.1
5.107	27.8	110.2	131.3	243.3	373.8	524.5
3.405	40.7	123.1	226.3	335.2	521.5	706.6
1.702	80.2	154.0	269.9	600.8	888.6	1126.2
1.362	100.1	212.6	278.9	698.1	1054.3	1341.2
1.021	132.8	228.7	318.7	845.7	1331.9	1690.5
0.681	198.4	235.9	401.2	912.9	1786.9	2098.2
0.34	391.1	374.7	496.1	1080.8	2592.4	3362.7
0.17	779.5	692.6	633.4	1831.9	2694.5	5937.2
0.153	868.7	772.8	811.6	1999.7	2845.1	6376.0
0.119	987.3	989.3	1035.9	2440.1	3529.5	7622.7
0.085	1234.3	1381.2	1284.0	3209.2	4610.3	9199.3
0.063	2012.1	1863.5	2137.6	4132	5857.5	10759.5
0.051	2197.5	2301.3	2417.7	4977.3	6878.2	12569.1
0.017	7128.9	7765.1	8741.2	13198.9	16276.8	21339.6

APPENDIX D

EXPERIMENT DATA FOR PAC

Table D. 1 - Shear Stress Values of PAC @ 60 °F

	Shear Stress (lb /100 ft^2)					
Shear	***0.25 lb/bbl***	***0.50 lb/bbl***	***0.75 lb/bbl***	***1.00 lb/bbl***	***1.25 lb/bbl***	***1.50 lb/bbl***
1021.38	10.5	19.0	27.1	37.7	43.7	56.8
510.69	7.2	13.0	18.4	26.3	30.6	40.4
340.46	5.4	9.9	14.4	20.8	24.2	32.6
170.23	3.3	6.2	8.9	13.5	15.7	21.8
102.138	2.2	4.0	6.5	9.5	11.3	15.8
51.069	1.3	2.2	3.7	6.1	6.7	10.0
34.046	1.0	1.7	2.4	4.1	4.7	7.2
17.023	0.6	0.9	1.5	2.2	2.6	4.1
10.214	0.4	0.7	1.0	1.8	2.0	2.9
5.107	0.4	0.4	0.7	0.9	1.5	1.8
3.405	0.4	0.3	0.5	0.7	0.9	1.6
1.702	0.3	0.3	0.4	0.4	0.7	1.1
1.362	0.3	0.3	0.3	0.4	0.5	0.9
1.021	0.3	0.3	0.3	0.3	0.5	0.9
0.681	0.2	0.2	0.3	0.3	0.4	0.8
0.34	0.2	0.2	0.2	0.3	0.4	0.6
0.17	0.2	0.2	0.2	0.3	0.4	0.6
0.153	0.2	0.2	0.2	0.3	0.4	0.5
0.119	0.2	0.2	0.2	0.2	0.4	0.5
0.085	0.2	0.2	0.2	0.2	0.3	0.5
0.063	0.2	0.2	0.2	0.2	0.3	0.4
0.051	0.2	0.2	0.2	0.2	0.3	0.4
0.017	0.2	0.2	0.2	0.2	0.3	0.4

Table D. 2 – Apparent Viscosity Values of PAC @ 60 °F

	Apparent Viscosity (cp)					
Shear Rate (s^{-1})	***0.25 lb/bbl***	***0.50 lb/bbl***	***0.75 lb/bbl***	***1.00 lb/bbl***	***1.25 lb/bbl***	***1.50 lb/bbl***
1021.38	5.7	9.3	14.5	17.9	20.3	26.7
510.69	6.5	12.2	17.3	24.7	28.5	37.9
340.46	7.1	14.0	20.3	29.3	33.9	45.9
170.23	8.2	17.5	25.1	38.0	44.1	61.5
102.138	9.4	19.0	30.4	44.6	52.5	74.1
51.069	10.3	20.5	34.9	49.8	63.1	93.8
34.046	11.7	23.4	37.1	57.3	66.6	101.4
17.023	14.3	25.2	43.2	62.8	69.9	116.2
10.214	17.6	31.8	47.7	73.4	86.7	136.6
5.107	25.3	38.4	61.5	85.4	99.2	142.7
3.405	32.4	48.0	74.8	95.9	119.4	163.1
1.702	56.0	75.9	98.9	125.8	135.5	183.6
1.362	66.3	91.0	108.8	137.4	143.7	194.1
1.021	85.5	118.3	131.6	161.2	170.8	212.4
0.681	122.8	171.9	181.4	217.8	227.8	235.8
0.34	242.0	289.3	342.2	407.9	460.6	503.2
0.17	481.5	534.3	649.8	716.8	798.7	868.8
0.153	530.9	634.9	709.7	799.2	826.8	947.0
0.119	679.0	743.3	896.7	994.8	1058.8	1219.7
0.085	837.1	1056.4	1253.9	1349.4	1477.7	1645.3
0.063	1253.2	1372.4	1682.1	1820.6	1884.3	1992.3
0.051	1536.3	1739.5	2076.5	2249.0	2475.9	2731.4
0.017	4593.3	5772.2	6320.2	6747.1	7141.2	7702.8

Table D. 3 - Shear Stress Values of PAC @ 100 °F

	Shear Stress (lb /100 ft^2)					
Shear Rate (s^{-1})	***0.25 lb/bbl***	***0.50 lb/bbl***	***0.75 lb/bbl***	***1.00 lb/bbl***	***1.25 lb/bbl***	***1.50 lb/bbl***
1021.38	9.5	16.9	24.9	37.3	38.9	55.7
510.69	6.8	11.4	16.6	23.1	29.7	38.0
340.46	5.3	9.1	13.2	20.6	22.7	30.0
170.23	3.1	6.0	8.7	12.3	15.2	21.4
102.138	2.0	3.6	5.8	8.5	11.1	15.8
51.069	1.2	2.1	3.3	5.7	6.5	8.8
34.046	0.9	1.6	2.4	3.9	4.7	6.4
17.023	0.5	0.9	1.4	2.0	2.4	3.7
10.214	0.4	0.7	0.9	1.6	1.8	2.6
5.107	0.3	0.4	0.6	0.9	1.4	1.7
3.405	0.3	0.3	0.5	0.6	0.8	1.5
1.702	0.2	0.3	0.4	0.4	0.7	1.0
1.362	0.2	0.3	0.3	0.4	0.5	0.9
1.021	0.2	0.3	0.3	0.3	0.4	0.8
0.681	0.2	0.2	0.3	0.3	0.4	0.8
0.34	0.2	0.2	0.2	0.3	0.4	0.6
0.17	0.2	0.2	0.2	0.3	0.4	0.6
0.153	0.2	0.2	0.2	0.3	0.4	0.5
0.119	0.2	0.2	0.2	0.2	0.3	0.5
0.085	0.2	0.2	0.2	0.2	0.3	0.4
0.063	0.2	0.2	0.2	0.2	0.3	0.4
0.051	0.2	0.2	0.2	0.2	0.3	0.4
0.017	0.2	0.2	0.2	0.2	0.2	0.3

Table D. 4 - Apparent Viscosity Values of PAC @ 100 °F

	Apparent Viscosity (cp)					
Shear Rate (s^{-1})	***0.25 lb/bbl***	***0.50 lb/bbl***	***0.75 lb/bbl***	***1.00 lb/bbl***	***1.25 lb/bbl***	***1.50 lb/bbl***
1021.38	5.1	7.7	12.8	15.2	17.7	23.8
510.69	5.9	10.5	14.7	20.3	24.2	34.1
340.46	6.0	11.3	16.4	26.1	27.5	41.8
170.23	7.1	15.1	20.8	31.2	39.2	56.0
102.138	7.5	16.0	26.4	40.6	44.6	60.0
51.069	8.2	17.8	30.4	44.8	51.1	78.8
34.046	10.1	20.6	33.8	48.3	53.3	89.2
17.023	12.3	22.9	36.3	52.1	61.5	95.3
10.214	15.5	28.0	42.9	66.1	77.2	110.6
5.107	21.8	30.7	52.9	71.7	80.4	124.1
3.405	27.9	42.7	59.8	77.7	97.9	148.4
1.702	48.7	63.0	81.1	86.8	112.5	157.9
1.362	57.7	73.7	91.4	109.9	127.9	165.0
1.021	73.5	102.9	114.5	137.0	152.0	176.3
0.681	111.7	137.5	159.6	180.8	182.2	214.6
0.34	217.8	257.5	273.8	367.1	405.3	427.7
0.17	390.0	427.4	571.8	609.3	632.8	695.0
0.153	424.7	539.7	612.9	655.3	735.9	814.4
0.119	604.3	594.6	780.1	895.3	942.3	1024.5
0.085	686.4	961.3	1090.9	1106.5	1300.4	1464.3
0.063	1065.2	1221.4	1396.1	1456.5	1601.7	1733.3
0.051	1382.7	1565.6	1682.0	1799.2	2079.8	2321.7
0.017	3858.4	4733.2	5742.1	6139.9	6641.3	7163.6

Table D. 5 - Shear Stress Values of PAC @ 120 °F

	Shear Stress (lb /100 ft^2)					
Shear Rate (s^{-1})	***0.25 lb/bbl***	***0.50 lb/bbl***	***0.75 lb/bbl***	***1.00 lb/bbl***	***1.25 lb/bbl***	***1.50 lb/bbl***
1021.38	9.0	15.9	23.8	37.1	36.4	55.1
510.69	6.6	10.6	15.7	23.6	29.2	36.5
340.46	5.2	8.7	12.7	19.5	22.0	28.5
170.23	3.1	5.9	8.6	11.7	15.0	21.1
102.138	1.9	3.5	5.4	7.9	11.0	15.8
51.069	1.1	2.0	3.2	5.6	6.4	8.2
34.046	0.8	1.5	2.4	3.8	4.7	6.0
17.023	0.5	0.8	1.3	1.9	2.3	3.5
10.214	0.4	0.7	0.9	1.5	1.8	2.4
5.107	0.2	0.4	0.6	0.9	1.3	1.6
3.405	0.2	0.3	0.5	0.6	0.8	1.5
1.702	0.2	0.3	0.3	0.4	0.7	1.0
1.362	0.2	0.2	0.3	0.4	0.5	0.9
1.021	0.2	0.2	0.3	0.3	0.4	0.8
0.681	0.2	0.2	0.2	0.3	0.4	0.8
0.34	0.2	0.2	0.2	0.3	0.4	0.6
0.17	0.2	0.2	0.2	0.2	0.4	0.5
0.153	0.2	0.2	0.2	0.2	0.4	0.5
0.119	0.1	0.2	0.2	0.2	0.3	0.4
0.085	0.1	0.2	0.2	0.2	0.3	0.4
0.063	0.1	0.2	0.2	0.2	0.2	0.4
0.051	0.1	0.2	0.2	0.2	0.2	0.3
0.017	0.1	0.2	0.2	0.2	0.2	0.3

Table D. 6 - Apparent Viscosity Values of PAC @ 120 °F

	Apparent Viscosity (cp)					
Shear Rate (s^{-1})	***0.25 lb/bbl***	***0.50 lb/bbl***	***0.75 lb/bbl***	***1.00 lb/bbl***	***1.25 lb/bbl***	***1.50 lb/bbl***
1021.38	4.7	6.9	14.0	13.9	16.3	22.6
510.69	5.3	9.6	18.2	18.1	22.0	32.7
340.46	5.5	10.0	24.5	24.6	24.1	39.8
170.23	6.5	13.8	27.5	27.9	36.7	53.2
102.138	6.6	14.5	38.6	38.6	40.5	54.0
51.069	7.3	16.5	42.5	42.5	45.1	70.8
34.046	9.3	19.1	44.1	43.8	46.2	82.6
17.023	11.3	21.9	46.8	46.9	57.6	85.1
10.214	14.4	26.0	62.2	62.3	72.4	96.1
5.107	19.9	26.8	65.3	64.5	70.4	113.5
3.405	25.7	40.2	68.3	69.1	86.5	140.2
1.702	45.2	56.7	66.7	67.9	100.9	147.7
1.362	53.2	65.3	96.6	96.6	120.0	153.9
1.021	67.4	95.0	124.9	124.9	142.6	155.5
0.681	106.1	119.8	162.8	161.2	158.1	204.6
0.34	206.4	241.6	346.7	346.7	376.9	391.1
0.17	342.9	375.6	558.7	555.5	547.4	602.9
0.153	370.0	490.6	585.6	583.4	687.6	738.2
0.119	565.8	520.3	845.6	848.6	884.1	938.7
0.085	613.3	913.8	985.1	977.8	1217.0	1392.8
0.063	971.2	1143.7	1263.5	1269.0	1464.6	1580.5
0.051	1308.2	1473.4	1587.8	1581.0	1875.7	2116.8
0.017	3479.9	4229.3	5845.4	5845.4	6376.4	6934.4